OXFORD

Cerebral Cortex, March 2017;27:2365–2384

doi:10.1093/cercor/bhw078
Advance Access Publication Date: 13 April 2016
Original Article

ORIGINAL ARTICLE

Homer1 Scaffold Proteins Govern Ca^{2+} Dynamics in Normal and Reactive Astrocytes

Lara Buscemi[1,2,†], Vanessa Ginet[1,3,†], Jan Lopatar[1,†], Vedrana Montana[4,5], Luca Pucci[1], Paola Spagnuolo[1,6], Tamara Zehnder[1], Vladimir Grubišić[5], Anita Truttman[3], Carlo Sala[7], Lorenz Hirt[2], Vladimir Parpura[5], Julien Puyal[1,3] and Paola Bezzi[1]

[1]Department of Fundamental Neurosciences, University of Lausanne, CH1005 Lausanne, Switzerland, [2]Stroke Laboratory, Neurology Service, Department of Clinical Neurosciences, University Hospital Centre and University of Lausanne, CH-1011 Lausanne, Switzerland, [3]Division of Neonatology, Department of Paediatrics and Paediatric Surgery, University Hospital Centre and University of Lausanne, CH-1015 Lausanne, Switzerland, [4]Department of Biotechnology, University of Rijeka, 51000 Rijeka, Croatia, [5]Department of Neurobiology, Center for Glial Biology in Medicine, Civitan International Research Center, Atomic Force Microscopy and Nanotechnology Laboratories, and Evelyn F. McKnight Brain Institute, University of Alabama at Birmingham, Birmingham, AL, USA, [6]Department of Pharmacy, Health and Nutritional Sciences, University of Calabria, Rende, Italy and [7]CNR Institute of Neuroscience and Department of Biotechnology and Translational Medicine, University of Milan, Milan, Italy

Address correspondence to Email: paola.bezzi@unil.ch

[†]Lara Buscemi, Vanessa Ginet, and Jan Lopatar contributed equally to this work.

Abstract

In astrocytes, the intracellular calcium (Ca^{2+}) signaling mediated by activation of metabotropic glutamate receptor 5 (mGlu5) is crucially involved in the modulation of many aspects of brain physiology, including gliotransmission. Here, we find that the mGlu5-mediated Ca^{2+} signaling leading to release of glutamate is governed by mGlu5 interaction with Homer1 scaffolding proteins. We show that the long splice variants Homer1b/c are expressed in astrocytic processes, where they cluster with mGlu5 at sites displaying intense local Ca^{2+} activity. We show that the structural and functional significance of the Homer1b/c–mGlu5 interaction is to relocate endoplasmic reticulum (ER) to the proximity of the plasma membrane and to optimize Ca^{2+} signaling and glutamate release. We also show that in reactive astrocytes the short dominant-negative splice variant Homer1a is upregulated. Homer1a, by precluding the mGlu5-ER interaction decreases the intensity of Ca^{2+} signaling thus limiting the intensity and the duration of glutamate release by astrocytes. Hindering upregulation of Homer1a with a local injection of short interfering RNA in vivo restores mGlu5-mediated Ca^{2+} signaling and glutamate release and sensitizes astrocytes to apoptosis. We propose that Homer1a may represent one of the cellular mechanisms by which inflammatory astrocytic reactions are beneficial for limiting brain injury.

Key words: astrocytes, Homer, intracellular Ca^{2+}, mGlu5, neuroinflammation

Introduction

A number of studies in the last decades establish a bidirectional glutamatergic communication between neurons and astrocytes (Parpura et al. 1994; Pasti et al. 1997; Bezzi et al. 1998; Wang, Lou, et al. 2006; Honsek et al. 2012). The interaction of synaptically released glutamate with G-protein-coupled receptors (GPCRs) in astrocytes, in particular with group I metabotropic glutamate receptors (mGlus), leads to transient elevations in intracellular Ca^{2+} levels (Porter and Mccarthy 1996; Pasti et al. 1997; Honsek et al. 2012). Glutamatergic Ca^{2+} signaling in astrocytes has been linked to the release of gliotransmitters that can modulate diverse physiological phenomena, including changes in blood vessel diameter (Iadecola and Nedergaard 2007; Gordon et al. 2008; Attwell et al. 2010; Giaume et al. 2010; Girouard et al. 2010) and synaptic transmission or plasticity (Araque et al. 1998; Fellin et al. 2004; Honsek et al. 2012; Min and Nevian 2012) suggesting that astrocytic mGlu signaling has a large impact on many aspects of brain physiology. However, the contribution of astrocytic Ca^{2+} signaling and the subsequent release of gliotransmitters to brain physiology has remained controversial. Recently, the activation of exogenous GPCRs in astrocytes failed to affect synaptic transmission (Fiacco et al. 2007; Agulhon et al. 2010) and the deletion of astrocytic inositol 1,4,5-trisphosphate receptor 2 did not enhance or lower baseline of hippocampal CA1 pyramidal neuron synaptic activity nor did it affect long-term potentiation (Petravicz et al. 2008; Agulhon et al. 2010) despite positive results reported at the same synapses (Fellin et al. 2004; Perea and Araque 2007; Henneberger et al. 2010). However, synaptic plasticity phenomena are exhibited in multiple forms and can be caused by various mechanisms, and in fact, certain forms of plasticity have been demonstrated to involve astrocytic signaling, such as the cholinergic-mediated plasticity in hippocampus and cortex (Takata et al. 2011; Navarrete et al. 2012) or the spike-timing-dependent plasticity in cortex (Min and Nevian 2012). Moreover, these seemingly disparate findings may result from the various conditions used in experimental approaches, some of them nonphysiological. Indeed, the vast majority of the current experimental techniques employed to evoke intra-astrocytic Ca^{2+} elevations do not reproduce the spatiotemporal aspects of physiological Ca^{2+} signaling. Recently, studies using chemical (Di Castro et al. 2011; Panatier et al. 2011) and genetically encoded (Shigetomi et al. 2010, 2013) Ca^{2+} sensors, have shown that Ca^{2+} signals in astrocytes may occur both in the form of global cytoplasmic increases and of local events along astrocytic processes. The discovery of localized Ca^{2+} events suggests that GPCR-mediated signaling in astrocytes is highly compartmentalized. It is likely that the GPCR signaling occurring in discrete subcellular regions can be uncorrelated with events that occur in the soma. The spatiotemporal characteristics of localized Ca^{2+} events in astrocytes may be subjected to a local independent modulation (Paukert et al. 2014) and thus be more heterogeneous and complex than previously assumed (Haustein et al. 2014; Rusakov et al. 2014; Volterra et al. 2014). However, the molecular and cellular mechanisms regulating localized Ca^{2+} events in astrocytes are not deciphered yet. Moreover, despite numbers of papers supporting the existence of mGlu5- and Ca^{2+}-mediated gliotransmission in the mature brain (Halassa and Haydon 2010; Araque et al. 2014), the functional role of mGlu5 in triggering glutamate gliotransmission has also been challenged, as the receptor expression is strongly downregulated in adult mice (Sun et al. 2013). These results raise the question of whether the Ca^{2+} events occurring in response to neural activity are limited to the postnatal period.

The existence of subcellular Ca^{2+} events implies a subcellular segregation of the signaling machinery responsible for such intracellular events. Association of mGlu5 with various scaffold proteins determines the activation state of the receptor and thereby constrains or enhances mGlu5-induced signal propagation. Scaffold proteins are thus crucial coordinators of plasma membrane receptor function. The most extensively studied are the interactions between mGlu5 and Homer, which determine the effects of mGlu5 on Ca^{2+} homeostasis (Ango et al. 2001), protein kinase signaling and behavior (Menard and Quirion 2012). The constitutively expressed long forms of Homer1b/c and the short, activity-dependent splice variant Homer1a, by switching on and off, respectively, the anchoring of the endoplasmic reticulum (ER) to plasma membrane receptors, increases the flexibility of a system in which the same signaling pathways provide different functional outcomes (Tu et al. 1998; Xiao et al. 1998, 2000; Fagni et al. 2000; Sala et al. 2001). The expression of Homer proteins and their functional consequences on the GPCR-mediated Ca^{2+} signaling in astrocytes has yet to be determined.

Here we report that mGlu1/5 signaling and the subsequent glutamate secretion by astrocytes are functionally controlled by Homer1 scaffold proteins. The long forms Homer1b/c are expressed in astrocytes from the first postnatal week to adult stages and, similarly to dendritic spines accumulate in subcellular regions where they cluster with mGlu5 receptors. *In vitro* studies show that Homer1b/c anchor ER tubules around sub-membrane microdomains, thus optimizing global and sub-plasmalemmal mGlu5-mediated Ca^{2+} events and glutamate exocytosis. Conversely, the short form Homer1a disrupts temporal correlation between Ca^{2+} signaling and glutamate exocytosis by preventing the ER tubules to approach the sub-plasmalemmal microdomains. We also examined the pathophysiological function of astroglial Homer1a in a rat model of neonatal cerebral hypoxia-ischemia (HI). In reactive astrocytes upregulation of Homer1a disrupts the Homer1b/c-mGlu1/5-ER microdomains and reduces both localized and global Ca^{2+} signals thus preventing glutamate release in response to mGlu1/5 activation. Hindering upregulation of Homer1a in vivo with a local injection of a siRNA downregulating Homer1a restores Ca^{2+} elevations and glutamate release in response to mGlu1/5 stimulation and sensitizes the reactive astrocytes to apoptosis. Overall, we identify Homer1 scaffold proteins as key members in the signaling pathway controlling Ca^{2+} in astrocytes both in physiological and pathological conditions closely associated with inflammatory processes.

Materials and Methods

Animal Models

All experiments concerning animals were performed in accordance with the Swiss Laws for the protection of animals or with the National Institutes of Health Guide for the Care and Use of Laboratory Animals and were approved by the Vaud Cantonal Veterinary Office or the Institutional Animal Care and Use Committee at the University of Alabama at Birmingham, respectively. Homer1 immunoreactivity was analyzed in glial fibrillary acidic protein (GFAP)-EGFP mice (Nolte et al. 2001) and in Sprague Dawley rat pups (Janvier, France). Hypoxia–ischemia (HI) was induced in 7-day-old 16 to 19 g Sprague Dawley male rats according to the Rice–Vannucci modification (Rice et al. 1981) of the Levine procedure (Levine 1960). Rat pups were anesthetized with 3% isoflurane and the right common carotid artery was isolated, double-ligated (Silkam, 5/0; B/BRAUN Aesculap, USA) and cut. After 2 h of recovery with the dam, pups were placed in a

humidified chamber at 35.5°C with 8% oxygen. To obtain a reproducible lesion volume, we selected a hypoxic period of 2 h, which produced substantial damage affecting most of the ipsilateral hemisphere (Ginet et al. 2009). After hypoxia, pups were returned to the dam until sacrifice. Sham-operated animals underwent the described anesthetic and surgical procedure without section of the common carotid artery.

Cell Culture

Enriched astrocytic cultures were prepared from cortices of 0- to 2-day-old Sprague Dawley rat or C57BL/6 mice pups, as previously described (Bezzi et al. 2001; Montana et al. 2004). Briefly, dissociated neural cells were initially plated into 25 cm^2 flasks and maintained in α-minimum essential medium (Life Technologies, USA) supplemented with fetal bovine serum (10%), L-glutamine (2 mM), D-glucose (20 mM), sodium pyruvate (1 mM), penicillin (100 IU/mL), streptomycin (100 μg/mL) and sodium bicarbonate (14 mM) and kept at 37°C in humidified 5% CO_2/95% air. After 14–18 days in culture, cells were purified for astrocytes (>99%) using an orbital shaker. Purified astrocytes were re-plated onto 35 mm dishes containing 12 mm round glass coverslips precoated with polyethyleneimine (1 mg/mL). Coverslips seeded with purified cells were kept in culture overnight, and then were submitted to a transfection procedure. All reported effects were tested using data originating from at least 3 independent cultures.

Plasmid Constructs and Transfections

The plasmid containing RCaMP1h (Akerboom et al. 2013) was kindly provided by Dr Loren Looger, (Howard Hughes Medical Institute, Ashburn, VA, USA). The Homer1a-YFP, Homer 1b-cyan fluorescent protein (CFP), and Homer1a-CFP plasmids (Sala et al. 2003) were kindly provided by Carlo Sala (Institute of Neurosciences, Milano, Italy). The ER-targeted GFP (ER-GFP) plasmid (Demaurex and Frieden 2003) was kindly provided by Nicolas Demaurex (University of Geneva, Geneva, Switzerland). The VGLUT1-pHluorin plasmid (Voglmaier et al. 2006) was kindly provided by Robert H. Edwards (University of California, San Francisco, CA). Each of these plasmids (0.5 μg for single transfection experiments or 0.25 μg for double transfection experiments) was transfected into primary rat or mouse cortical astrocytes cultures with Lipofectamine2000 (Life Technologies) or TransIT 293 (Mirus, USA), respectively, following the manufacturers specifications. Astrocytes were imaged in experiments 3 days post-transfection.

In Vitro siRNA Interference

The Homer1a interference was performed using custom designed fluorescently labeled Accell siRNAs (Dharmacon-Thermo Fisher Scientific). The Accell siRNA is a novel chemically modified siRNA that allows rapid and efficient in vivo and in vitro delivery and knockdown in the absence of transfection reagents. We used siRNAs targeting the beginning of the unique to Homer1a 3′-UTR, siRNA1: 5′-Cy3-GGUGGAUAAUUGGAAGUCAUU-3′, and the small differential region between Homer1a and the long splice variants Homer1b/c on the open reading frame, siRNA2: 5′-Cy3-CAGC AATCATGATTAAGTA-3′. Both siRNAs had been previously used to knockdown Homer1a in neurons (Moutin et al. 2012; Serchov et al. 2015). A nontargeting DY-547-labeled Accell Red siRNA (Dharmacon-Thermo Fisher Scientific) was used as a control in all siRNA experiments. Accell siRNAs were delivered to primary cortical astrocytes in low-serum medium (1.5% FBS). Cells were cultured for 2–3 additional days after the addition of 1 μM siRNA, according to the manufacturer's instructions, then treated if indicated, lysed, and subsequently analyzed for mRNA and protein expression. siRNA treatment efficiency and specificity were validated by detection of red-labeled cells in treated cultures and by quantification of Homer1a mRNA and Homer1a protein expression levels.

In Vivo Stereotaxic Intracerebroventricular siRNA Delivery

For in vivo injections, endotoxin free Accell Red Non-targeting control siRNA and the in vitro tested anti-Homer1a siRNA2: 5′-Cy3-CAGCAATCATGATTAAGTA-3′ Accell siRNA (Dharmacon-Thermo Fisher Scientific) were used. The rat pups were placed in a stereotaxic frame under isoflurane anesthesia (2.5–3%) 5 days after the surgery. The siRNAs (2 μg/μL) dissolved in Accell siRNA delivery media (Dharmacon-Thermo Fisher Scientific) were intraventricularly injected in the damaged hemisphere with a Hamilton syringe fitted with a 33-gauge needle (0.5 mm anteriorly, 1.5 mm laterally, 3.5 mm deep, relative to Bregma) at a rate of 1 μL/min (total volume of 5 μL). The needle was left in place for 5 min after the injection and then slowly withdrawn. Afterwards, the pups were allowed to recover from the surgery and returned to the dam. The siRNA delivery and localization in astrocytes was verified by visualization of the red tag present on the siRNAs.

Human Newborn Brain Specimens

Human brain tissues were obtained from autopsied newborns provided by the Institute of Pathology of the University of Lausanne. Autopsies were performed for medical and legal reasons. Informed consent for tissue collection was obtained from the parents, and the local ethical committee approved the use of the anonymized specimens. Selection was made retrospectively from the death reports of the neonatology unit between 2001 and 2009. We selected newborns who died after birth due to severe hypoxic–ischemic encephalopathy (HIE). The criteria for HIE cases were: newborns at or near term (35–37 weeks gestation), with severe perinatal asphyxia, and clinical HIE according to Sarnat grade III (Sarnat and Sarnat 1976). Control cases were newborns at or near term (35–37 weeks of gestation) with life-incompatible conditions whose autopsies did not indicate brain injury (cerebral malformations and genetic anomalies were excluded). After fixation in 10% buffered formalin for 3 weeks, the samples were embedded in paraffin, 3-μm thick sections were cut and then immunohistochemistry was performed as described previously (Ginet et al. 2014).

Epifluorescence/Total Internal Reflection Fluorescence

After transfection, coverslips were mounted in an open laminar flow perfusion temperature-controlled incubator (Harvard Apparatus, USA) mounted on the stage of a Zeiss Axiovert 200 fluorescence inverted microscope modified for total internal reflection fluorescence (TIRF) and epifluorescence (EPI) experiments (Visitron Systems, Switzerland) (Marchaland et al. 2008). The experimental chamber (250 μL volume) was kept at 37°C and perfused with Krebs-Ringer HEPES (KRH) buffer containing (in mM) 120 NaCl, 3.1 KCl, 2 $MgCl_2$, 1.8 $CaCl_2$, 1.25 NaH_2PO_4, 25 HEPES-Na (buffered to pH7.4), 4 glucose at a rate of 1–1.5 mL/min. For Ca^{2+} imaging experiments, cells transfected or not transfected were loaded with 5 μM Fluo-4 AM (Life Technologies) for 15 min in the presence of 0.02% pluronic F-127 (Life Technologies) at room temperature in the dark in KRH buffer, pH7.4, and then de-esterified for 10–15 min before imaging. The stimulus

((RS)-3,5-dihydrophenylglycine [DHPG]; Tocris Bioscience, USA) was applied rapidly (2 s) via a software-controlled microperfusion fast-step device (100 µL/min; Warner Instruments, USA). In TIRF/EPI experiments, EPI and TIRF were alternated in real time for whole-cell Ca^{2+} measurements in individual cells, in basal conditions and upon stimulation with DHPG. By imaging with excitation light at 488 nm generated by 488 nm laser (20 mW; Laserphysics) or by polychromator illumination system (Visichrome), the fluo4 signal was recorded at 10 Hz through 100× objective lens (Zeiss; α-plan FLUAR 100×, 1.45 NA). Traces corresponding to Ca^{2+} TIRF and EPI were calculated by placing a single ROI around the whole-cell perimeter of CFP-expressing or nontransfected cells and expressed as background-subtracted $\Delta F/F_0$. TIRF/EPI video images were digitized with MetaFluor and were analyzed with MetaMorph software (Universal Imaging, USA). In TIRF experiments, Ca^{2+} events were monitored as fast as possible (20 Hz) and analysis was restricted to 10 regions of interest (ROIs) per cell located at different subdomains (i.e., in the processes and cell body). Traces corresponding to Ca^{2+} TIRF were calculated in CFP-expressing or nontransfected cells, expressed as background-subtracted $\Delta F/F_0$, counted in each frame, and plotted against time to obtain their temporal distribution. Each histogram represents the number (mean ± SD) of sub-plasmalemmal Ca^{2+} events counted in a 50 ms-long frame. For TIRF experiments on exocytosis processes cultured astrocytes were prepared as previously described and plated on glass coverslip and transfected 6 days later with VGLUT1-pHluorin or ER-GFP constructs (Marchaland et al. 2008). After transfection, coverslips were mounted in the open laminar flow perfusion incubator as described above.

Immunostaining

For rat and mouse tissues, pups were deeply anesthetized with an i.p. injection of 150 mg/kg sodium-pentobarbital and perfused intracardially with 4% paraformaldehyde in 0.1 mol/L PBS), pH 7.4. Immunohistochemistry staining was performed on 18 µm cryostat sections.

For human tissue, paraffin-embedded sections were first deparaffinized and after antigen retrieval and blocking in PBS with 15% donkey serum sections were incubated with primary antibodies in 1.5% donkey serum overnight at 4°C, as described previously (Ginet et al. 2014).

For immunoperoxidase labeling, sections were treated for 20 min in 0.3% H_2O_2 in methanol to quench endogenous peroxidases, preincubated in 15% serum and 0.3% Triton X-100 in PBS and then incubated overnight with the primary antibody in 1.5% serum and 0.1% Triton in PBS. Sections were rinsed in PBS, incubated with the biotinylated secondary antibody (Jackson ImmunoResearch Laboratories), detected using the avidin–biotin–peroxidase kit (VECTASTAIN Elite ABC Kit Vector, PK-6200) and then developed by incubation with 3–3′-diaminobenzidine (DAB, Roche, 11718096001) substrate solution until the desired intensity of staining was obtained. The sections were finally dehydrated in graded alcohols and mounted in Eukitt mounting medium. For immunofluorescence labeling, the sections were preincubated in 15% serum and 0.3% Triton X-100 in PBS and then incubated overnight at 4°C with the primary antibody in 1.5% serum and 0.1% Triton in PBS, washed in PBS, and incubated in fluorophore-coupled secondary antibody (Alexa Fluor 488 or Alexa Fluor 594 from Molecular Probes) at room temperature. The sections were then rinsed in PBS and mounted in Fluor-Save™ mounting medium (Calbiochem, #345-789-20). The antibodies used were as follows: anti-Homer1b/c rabbit polyclonal (sc-25271) and anti-Homer1a (sc-8922) antibodies from Santa Cruz Biotechnology; anti-GFAP mouse monoclonal (#G3893) and anti-S100β mouse monoclonal (#S2532) antibodies from Sigma; and anti-mGlu5 rabbit polyclonal antibody (#AB5675) and anti-cleaved (active) caspase-3 rabbit polyclonal (#AB3623) from Millipore.

Images from immunoperoxidase staining were taken with an Axioplan2 microscope (Carl Zeiss, Germany). Confocal laser microscopy was performed with a TCS SP5 RS—DM6000 confocal scanning microscope (Leica, Germany). Unless otherwise noted, representative confocal images are displayed as single planes. For double labeling, immunoreactive signals were sequentially acquired in the same section. Images were processed with Fiji/ImageJ software (NIH, USA).

For cultured astrocytes, to estimate cell surface expression of the mGluR5 receptors and its regulation by Homer1 proteins, cells were transfected with Homer1a-CFP or Homer1b-CFP. 24 h after transfection cells were briefly washed with PBS and were gently fixed in 100% methanol at 4°C for 20 min and incubated with mGlu5 antibody for 30 min at 37°C and with the secondary antibody 2 h at room temperature. Following incubation with anti-mGlu5 antibody, cultures were mounted with PBS and imaged with TIRF. Primary and secondary antibodies were applied in GDB buffer (30 mM phosphate buffer, pH 7.4, containing 0.2% gelatin, 0.3% Triton X-100, and 0.8 M NaCl).

For active caspase-3 analysis, z-stacks of images with 1 µm vertical spacing were taken at 40× in the peri-lesion area using confocal microscopy. At least, 3 series of images per animal were taken. Immunopositive cells for active caspase-3, GFAP and active caspase-3/GFAP were counted. Counts were performed using Image J software with the investigator blinded to the treatment group.

Ca^{2+} Imaging on Acute Slices

Juvenile rats that were subjected to sham-operation or to ischemia were used for preparation of acute slices. Seven days after the intervention rats were cervically dislocated and decapitated and their brains were rapidly removed and immersed in ice-cold cutting solution that contained (in mM) 2 $CaCl_2$, 11 $MgSO_4$, 125 NaCl, 3 KCl, 26 $NaHCO_3$, 1.3 NaH_2PO_4, and 10 glucose, pH = 7.4. Coronal slices (250 µm) were cut using a vibratome and immediately transferred to oxygenated (5% CO_2, 95% O_2) standard aCSF (same composition as cutting solution except for 1 mM $MgSO_4$). Slices were incubated in aCSF for at least 1 h at 34°C before 60 min incubation with the calcium indicator Fluo-4 AM (10 µM, 0.1% pluronic acid) and sulforhodamine 101, a specific marker for astrocytes (SR 101, 2 µM) (Nimmerjahn et al. 2004). After the loading, slices were subjected to a 20 min wash in oxygenated aCSF at 34°C. The slices were then placed on a perfusion chamber mounted on the prewarmed (34°C) TCS SP5 RS—DM6000 confocal scanning microscope stage and perfused with warm oxygenated aCSF. DHPG (100 µM) and ionomycin (10 µM), a Ca^{2+} ionophore, were added to the perfused aCSF. Imaging was performed using a 20× water-immersion objective (NA 0.5) at a 0.5 Hz rate in a single optical plane in sequential acquisition mode, using 488 nm laser excitation for Fluo-4 and 561 nm for SR101. The duration of the experiments was restricted to 200–300 s.

Data Processing

Global Ca^{2+} Events Detection and Analysis

Time-series images were corrected for lateral drift (TurboReg plugin, ImageJ) and digitally filtered (Hybrid 3D Median filter,

ImageJ) before analysis. Ca^{2+} transients were analyzed by plotting the intensity of ROIs placed around the soma and large processes over time. Data are expressed as $\Delta F/F_0 \pm$ SEM (%) in which ΔF represents the change of fluorescence, while F_0 represents the fluorescence of the cell at rest. $\Delta F/F_0$ values obtained for the $[Ca^{2+}]_i$ (Fluo-4 emission signal) were normalized to the $\Delta F/F_0$ values corresponding to the SR101 red channel. Data were further normalized against the maximal response to 10 μM ionomycin ($\Delta F/F_0$, % vs. ionomycin). Cells were considered as responding when, in response to agonist application, displayed increases in $[Ca^{2+}]_i$ higher than 2 standard deviations above baseline. The baseline was measured as the mean intensity of the frames preceding the application of agonist. Ca^{2+} wave amplitudes were measured by calculating the difference between pre- and post-agonist stimulation followed by normalizing to the pre-agonist intensity levels ($\Delta F/F_0$). Data analysis was done using R software (R Project for Statistical Computing, http://www.r-project.org/) and statistical tests were run in GraphPad Prism5.0 using parametric or nonparametric tests as appropriate.

Localized Ca^{2+} Events Detection and Analysis

Astrocytes for localized Ca^{2+} detection were identified using SR101, and were carefully chosen based on their low basal Fluo-4 AM fluorescence, their ability to respond to DHPG, and provided their cell body and a main process lied in the focal plane. Localized Ca^{2+} events were then detected in about 1 μm^2 ROIs placed on several subdomains (cell body and main process) of the astrocytes. At least 5 ROIs were chosen per astrocyte. A signal (measured as $\Delta F/F_0$) was taken into account provided the amplitude exceeded 3 times the background noise. Background noise was calculated by averaging three 5s-long time intervals without obvious Fluo-4 activity in basal conditions. ROIs were chosen using Leica Application Suite and signal was further analyzed and plotted with Origin 8 (OriginLab Corporation, Northampton, USA). Amplitudes and frequencies of localized Ca^{2+} signals were measured in the somata and processes of normal and activated astrocytes in the absence (basal) and presence (DHPG) of group I mGluR agonist DHPG. The peaks were recognized by the Spike 2 software (version 5, CED, Cambridge, UK) and were taken into account based on the following criteria: (1) background noise was calculated for each ROI prior to DHPG application, (2) any deflection larger than 3× the background noise was considered a spike, (3) only deflections between 2 adjacent time points were taken into account.

Glutamate Measurements

Cultured astrocytes: Ca^{2+}-dependent glutamate release from cultured astrocytes was measured using the L-glutamate dehydrogenase (GDH)-linked assay, as previously described (Hua et al. 2004; Montana et al. 2004; Lee et al. 2008). When released to the extracellular space, glutamate is converted by GDH to α-ketoglutarate with the concomitant reduction of the bath-supplied coenzyme NAD^+ to NADH, the latter being a fluorescent product when excited by UV light. Astrocytes were bathed in external solution containing (in mM): 140 NaCl, 5 KCl, 2 $CaCl_2$, 2 $MgCl_2$, 5 glucose, and 10 HEPES (pH 7.4) supplemented with NAD^+ (1 mM; Sigma-Aldrich, USA) and GDH (~53–137 IU/mL; Sigma-Aldrich, cat. No. G2626, USA) (pH = 7.4). To evoke an increase in cytosolic Ca^{2+} levels of solitary astrocytes (see Supplementary Information) and consequential exocytotic glutamate release, astrocytes were mechanically stimulated using glass pipettes filled with external solution, as described in detail elsewhere (Hua et al. 2004). To achieve a reproducible strength of the contact between the pipette and the solitary astrocytes, pipette resistance was monitored using a patch-clamp amplifier (PC-ONE; Dagan, USA) (Reyes et al. 2013). Every experiment was preceded by a sham run on astrocytes bathed in solution lacking GDH and NAD^+, which was used to correct for photo-bleaching and background subtraction. After correction, all imaging data were expressed as $\Delta F/F_0$ (%), in which ΔF represents the change of fluorescence, while F_0 represents the fluorescence level surrounding the astrocyte, immediately and laterally of its soma, before mechanical stimulation. All experiments were done at room temperature using an inverted microscope (TE 300; Nikon, Japan) equipped with differential interference contrast and wide-field fluorescence illumination. NADH fluorescence was visualized using a standard 4′6-diamidino-2-phenylindole filter set (Nikon). Images were captured through a 40× SFluor objective (1.3 NA; Nikon) using a CoolSNAP-HQ cooled CCD camera (Photometrics, USA) driven by V++ imaging software (Digital Optics, New Zealand). For time-lapse image acquisition, a camera and an electronic shutter (Vincent Associates, USA) inserted in the excitation pathway were controlled by software. All raw data/images had their pixel intensities within the camera's dynamic range (0-4095).

For the glutamate release analysis, the $\Delta F/F_0$ of the test groups (RCaMP1h ± Homer1a) were ranked and normalized to control (RCaMP1h) in order to allow comparisons between experimental batches and accommodate for variations in GDH concentration and culture conditions. Resulting proportions were expressed as a median ± interquartile range.

Acute slices: efflux of endogenous glutamate from cortical slices was monitored by the use of Glutamate Assay Kit (Sigma-Aldrich), according to the manufacturer's directions. Briefly, cortical slices were lodged in a cuvette inside a bath at 37°C under stirring in a buffer containing (in mM) NaCl 120, KCl 3.1, NaH_2PO_4 1.25, HEPES-Na 25, glucose 4, $MgCl_2$ 1, $CaCl_2$ (pH 7.4), added with plasmalemmal glutamate uptake blocker DL-*threo*-β-benzyloxyaspartate (TBOA, 100 μM) and of bafilomycin A1 (BafA1, 2 μM), a blocker of V-ATP-ase and hence vesicular release from neuronal terminals (Zhou et al. 2000); of note, BafA1 collapses vesicular proton gradient necessary for vesicular loading with transmitter. The effect of BafA1 on vesicular exocytosis was assessed by high K^+ (KCl, 20 mM) 2 h after the exposure. KCl or DHPG (100 μM) were added directly in the cuvette through a microsyringe. Release was quantified by referring to standard curves constructed with exogenous glutamate and normalized for the protein content of each sample.

Statistical Analysis

Statistical tests were run in GraphPad Prism (GraphPad, USA), GB-Stat 6.5 software (Dynamic Microsystems Inc., Silver Spring, MD, USA). Data were analyzed for normality and statistical tests were run accordingly. Significance is declared at $P < 0.05$.

Results

Homer1b/c is Expressed in Developing Astrocytes

To investigate the potential role of scaffold proteins in the regulation of Ca^{2+} excitability in astrocytes, we examined the expression of Homer1 in cortical tissues of rodents during postnatal development (Fig. 1). Immunohistochemistry analyses were performed by using well-characterized antibodies (Tappe et al. 2006) (Fig. 1, Supplementary Fig. 1A). Immunohistochemistry showed that Homer1b/c and S100β, a marker of astrocytes, were coexpressed in cortical tissue from the first postnatal week (Fig. 1A),

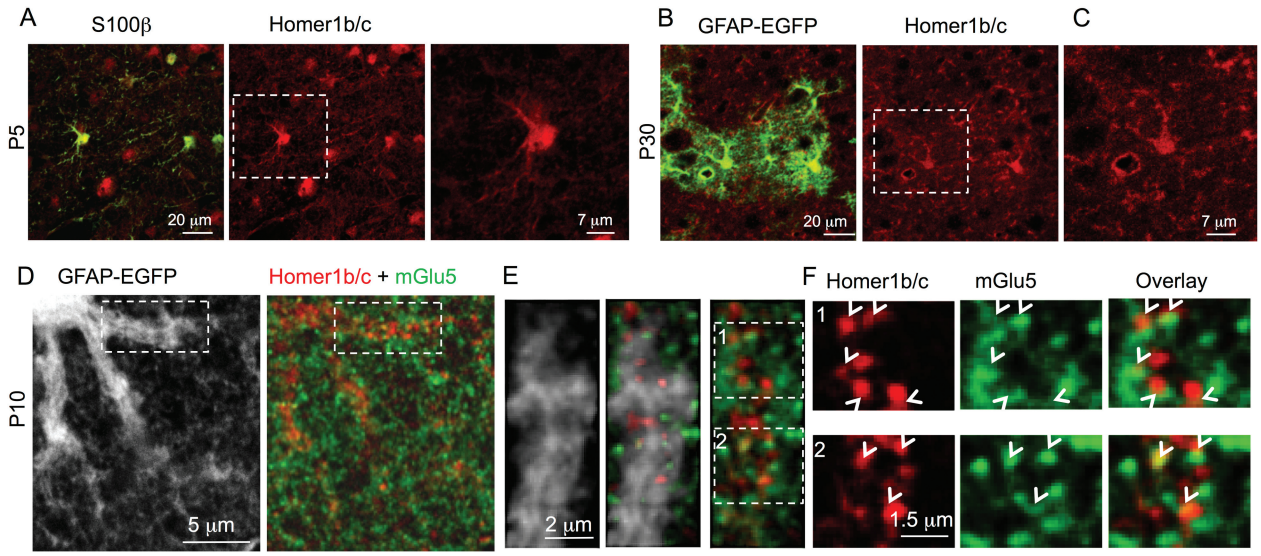

Figure 1. Homer1b/c are expressed in astrocytes and their immunoreactivity overlaps with mGlu1/5 immunoreactivity. (*A*, *B*) Homer1b/c are expressed in cortical astrocytes across species. (*A*) P5 rats, a diffuse staining for Homer1b/c (red) is present within cell bodies and processes of cortical S100β-positive cells (green). (*B*) P30 GFAP-EGFP mice, cortical astrocytes (green) largely express Homer1b/c (red) in their cell bodies and processes. (*C*) High magnification of an astrocyte in *B*. (*D*) Double labeling of P10 GFAP-EGFP astrocytes. The punctate staining for Homer1b/c (red) observed in juvenile mice partially colocalized with mGlu5 (green) staining in the large astrocytic processes; left panel shows a single plane of EGFP fluorescence expressed under the GFAP promoter. Boxed region marks large astrocytic process shown in *E*–*F*. (*E*, *F*) High magnification of the Homer1b/c and the mGlu1/5 puncta on the large astrocytic process (box in *D*) shows an overlap of the 2 signals (*F*, arrowheads).

a timing in the postnatal development coinciding with the active cortical synaptogenesis (Eroglu and Barres 2010) and with highest expression of mGlu5 in astrocytes (Sun et al. 2013). At P30, a vast majority of cortical astrocytes expressed low but still detectable levels of mGlu5 (Supplementary Fig. 1*B*) and were positive for Homer1b/c (~90%), the signal of which was readily recognizable in the soma and large astrocytic processes (Fig. 1*B*,*C*) with some variability in the intensity of the signal among astrocytes. For Homer1a, the short splice variant of Homer1, the immunolabeling signal during postnatal development was, however, undetectable in the neuropil and in astrocytes (Supplementary Fig. 1*C*). Having established that developing astrocytes express Homer1b/c, we then set to determine its distribution with respect to mGlu5. At first, we examined by electron microscopy the expression and distribution of mGlu5 in astrocytic processes using both immunoperoxidase and immunogold labeling. Ultrastructural analysis, performed at P14, reliably showed mGlu5 immunoreactivity both in the large and fine perisynaptic processes of cortical astrocytes (Supplementary Fig. 1*D*–*E*). Subsequently, we double labeled juvenile cortices (P10) of GFAP-EGFP mice for Homer1b/c and mGlu5. At P10, at high magnification Homer1b/c exhibited a punctate distribution in the neuropil (Fig. 1*D*–*F*), consistent with previous findings showing the localization of Homer1b/c within dendritic spines (Brakeman et al. 1997; Inoue et al. 2004; Sala et al. 2005). The puncta did not outline obvious cellular structures but were clearly and consistently associated with EGFP-positive profiles of astrocytes in tissue obtained from transgenic GFAP-EGFP mice (Fig. 1*D*). For colocalization analysis, considering that both Homer1b/c and mGlu5 are expressed in spines and that astrocytic processes are intimately associated with synapses during the early postnatal developmental stage (Halassa et al. 2007; Clarke and Barres 2013), we excluded the peripheral astrocytic processes (<100 nm in diameter/length; Lavialle et al. 2011) and instead focused on the main astrocytic processes (≥2 μm in diameter; Schubert et al. 2011). Colocalization was performed at very high magnification by inspecting the Homer1b/c and mGlu5 puncta located inside of a given astrocytic process (Fig. 1*E*–*F*, Supplementary Fig. 2). Detailed analysis performed by tracing the intensity profile (Marchaland et al. 2008) on top of any given red punctum, representing Homer1b/c, and its closest green punctum, representing mGlu5, defined that the scaffold protein completely overlapped with the receptor in 35% of cases (Supplementary Fig. 2*B*). The most frequent pattern, however, was that Homer1b/c and mGlu5 puncta were located side by side, with some overlap of their puncta (about 37% of cases, Supplementary Fig. 2*B*). Considering the relatively small volume of the main astrocytic processes, we concluded that the scaffold protein and the receptor were forming clusters of ~1 μm of width, estimated from the full-width-half-max of the overlapping line-scans (Supplementary Fig. 2*B*,*C*), which delimited near-membrane microdomains.

Homer Proteins Govern Recruitment of ER Tubules in the sub-plasmalemmal Domains of Astrocytes and Modulate Localized Ca^{2+} Events

After having demonstrated that Homer1b/c is expressed in astrocytes, the next step was to investigate their functional role. Since the overexpression of Homer1b/c in cultured neurons has been shown to induce IP_3R and ER recruitment in dendritic spines (Sala et al. 2001, 2005) together with the surface clustering of mGlu5 (Kammermeier 2006), we posit that Homer1 proteins have a role in the spatial arrangement of mGlu1/5 and ER tubules in astrocytes. To verify this hypothesis, cultured astrocytes were transfected with DNA constructs encoding for fluorescently tagged Homer1b or Homer1a (Sala et al. 2005). Upon expression of exogenous Homers tagged with CFP astrocytes were fixed while preserving plasma membrane integrity and immunostained for mGlu5. The analysis of the expression and membrane distribution of mGlu5 was performed by taking advantage of TIRF microscopy, which uses evanescent wave illumination to excite only plasmalemma and restricted sub-membrane space,

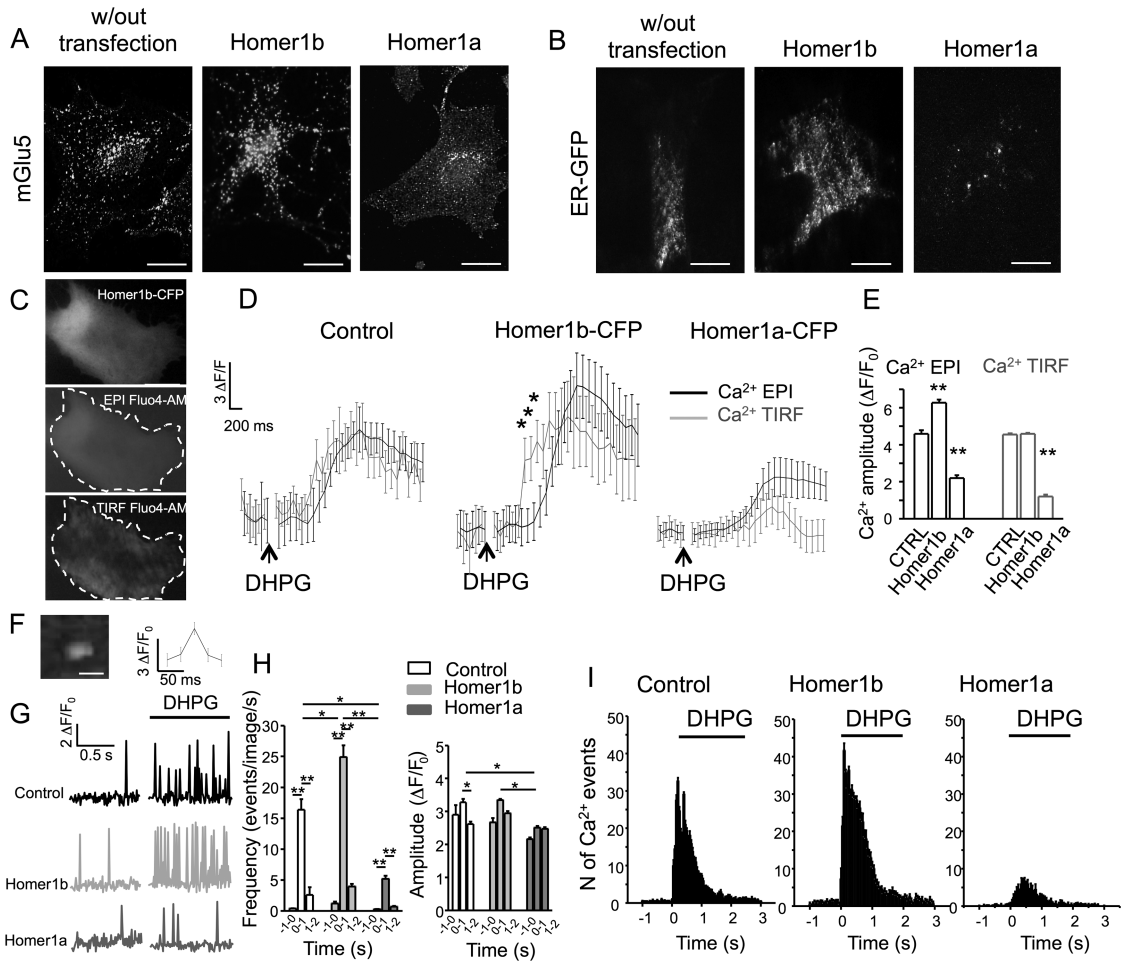

Figure 2. Functional role of Homer1 isoforms in regulation of Ca^{2+} microdomains in cultured astrocytes. (*A*, *B*) TIRF images of mGlu1/5 and ER distributions in astrocytes not transfected or transfected with Homer1a-CFP or Homer1b-CFP. (*A*) Overexpression of Homer1b or Homer1a induces clustering and declustering of mGlu1/5, respectively. Cultured astrocytes are transfected with Homer1b-CFP or Homer1a-CFP and subsequently immunostained for mGlu5. TIRF illumination reveals a sub-plasmalemmal distribution of mGlu5. Larger clusters of the receptor are present in Homer1b-transfected cells compared with nontransfected cells (middle and left, respectively). The distribution of the receptor is more diffuse when cells are transfected with Homer1a (right). Scale bars: 20 μm (*B*) Overexpression of Homer1b or Homer1a induce association and dissociation of ER tubules with the plasma membrane. Cultured astrocytes are transfected with only ER-GFP (left) or co-transfected with ER-GFP and Homer1b-CFP or Homer1a-CFP (middle or left, respectively). Under TIRF illumination, Homer1b cotransfected cells exhibit an increase in GFP fluorescence (middle), while the GFP florescence is decreased in Homer1a cotransfected cells. Scale bars: 20 μm (*C–E*) Global and sub-membrane intracellular Ca^{2+} concentration $[Ca^{2+}]_i$ induced by stimulation with 3,5-dihydroxyphenylglycine (DHPG). (*C*) Cultured astrocytes transfected with Homer1b-CFP (top panel) or Homer1a-CFP are incubated for 20 min with 5 μM Fluo4-AM and illuminated with epifluorescence (EPI, middle panel) for global Ca^{2+} imaging or with TIRF illumination (lower panel) for sub-membrane, local Ca^{2+} imaging. Scale bars: 20 μm (*D*) Traces corresponding to Ca^{2+}-EPI or Ca^{2+}-TIRF in CFP-expressing or nontransfected (Control) cells before and after local application of DHPG (100 μM, 2 s) were plotted as background-subtracted $\Delta F/F_0$. Note faster response of sub-membrane $[Ca^{2+}]_i$ of Homer1b-transfected cells (middle). *$P < 0.05$, one-way ANOVA. (*E*) The amplitude of the global $[Ca^{2+}]_i$ response to DHPG (Ca^{2+} EPI, left) is significantly larger in Homer1b/c and decreased in Homer1a-overexpressing cells in comparison with control nontransfected cells (CTRL). The amplitudes of the sub-membrane $[Ca^{2+}]_i$ responses to DHPG (Ca^{2+} TIRF, right) are significantly decreased in Homer1a-transfected cells while remain unchanged in Homer1b-transfected cells. **$P < 0.01$, one-way ANOVA. Group sample sizes, $n = 8$. (*F–I*) Properties of localized Ca^{2+} events. (*F*) High magnification image of a sub-membrane Ca^{2+} event, with a typical $\Delta F/F_0$ trace. Scale bar: 2 μm (*G*) Three representative example traces of localized Ca^{2+} events illustrate what is summarized in (*H*). In Homer1a-overexpressing cells there is a cessation of spontaneous Ca^{2+} spiking activity compared with control or Homer1b-overexpressing cells. Group I mGlu activation only marginally increases the frequency of events in Homer1a-overexpressing cells, while a large increase in spiking frequency is observed in controls and Homer1b-overexpressing cells. Also, Homer1a-overexpressing cells exhibit reduction in amplitude. (*H*) Frequency (left) and amplitude (right) of localized Ca^{2+} events, grouped into three 1-second bins, one before (-1-0) and 2 after the DHPG application. **$P < 0.01$,*$P < 0.05$, one-way ANOVA (*I*) Before and after the local application of DHPG, the sub-membrane Ca^{2+} events occurring in 100 ms-long frames are counted and plotted (mean ± SD for each histogram bar) to obtain their temporal distribution ($n = 5$ cells for each of the groups). The overexpression of Homer1a results in a dramatic reduction of the number of localized events of Ca^{2+}.

allowing monitoring of membrane-bound mGlu5 with a very high resolution (Lee et al. 2007). The effects of Homer proteins on the mGlu5 distribution were quite strong; the vast majority of astrocytes overexpressing Homer1b showed mGlu5 clusters at the plasma membrane, whereas cells overexpressing Homer1a showed a relatively diffuse distribution of the receptor (Fig 2A). Nontransfected control cells showed a pattern similar to those overexpressing Homer1b but with a less pronounced surface clustering of the receptor. These data are in line with the fact that nontransfected cells express significant levels of Homer1b/c (Supplementary Fig. 4A) and with previous reports in neurons (Ango et al. 2000; Kammermeier 2006) and heterologous expression systems (Coutinho et al. 2001) and suggest a similar regulation of group I mGlus by Homer proteins across various cell types. The effect of Homer1 proteins on the cellular distribution of ER tubules was then monitored in living cells expressing fluorescent

constructs for Homer1b or Homer1a together with ER-GFP (Demaurex and Frieden 2003; Marchaland et al. 2008). The fluorescent ER in control cells and cells overexpressing Homer1b appeared as discrete structures, consisting of the tubules closely distributed near the plasma membrane (Fig. 2*B*). Conversely, in the presence of Homer1a fluorescent ER was almost undetectable under TIRF illumination (Fig. 2*B*). This result is consistent with the effect of Homer1a on neuronal spines where the disruption of the structural link between mGlu1/5 and ER prevented the ER tubules to reach the very near vicinity of the plasma membrane (Sala et al. 2005). We then studied the effects of Homer proteins on mGlu1/5-mediated sub-plasmalemmal and intracellular Ca^{2+} signaling. Taking advantage of epifluorescence (EPI) and TIRF illuminations to evaluate the global and the near-membrane Ca^{2+} responses (Jaiswal and Simon 2007; Marchaland et al. 2008; Shigetomi et al. 2010), respectively, we examined the ability of the group I mGlu specific agonist 3,5-dihydroxyphenylglycine (DHPG) to elevate Ca^{2+} in control astrocytes or in cells overexpressing Homer1b or Homer1a (Fig. 2*C*). In control astrocytes, DHPG-induced Ca^{2+} elevations both in the bulk cytosol and near-membrane, with similar kinetics and amplitudes (Fig. 2*D*). Both signals started within 1.6 s after the stimulus and reached the maximum peak in 3 s. In the presence of Homer1b, the amplitude of the EPI signal was significantly increased (+36.5%, Fig 2*E*) with respect to the control conditions; the kinetics of TIRF signals, in particular, were significantly accelerated (Fig. 2*D*). In the presence of Homer1a, however, the amplitudes of both EPI and TIRF signals were significantly reduced (−51% EPI and −73.5% TIRF, Fig. 2*E*). Interestingly, this remarkable effect of Homer1a was not limited to signaling coupled to mGlu1/5, as similar alterations were detected by challenging astrocytes both with stromal cell-derived factor-1 alpha (SDF-1α), a specific agonist of the C-X-C chemokine receptor type 4 (CXCR4 receptor) known to stimulate Ca^{2+}-dependent release of glutamate from astrocytes (Bezzi et al. 2001), and with mechanical stimulation (Supplementary Fig. 3), which relies on the recruitment of Ca^{2+} from the ER store (Hua et al. 2004). In a parallel series of TIRF experiments, we studied the effects of Homer proteins on spatially confined sub-plasmalemmal Ca^{2+} events (Marchaland et al. 2008; Santello et al. 2011) (Fig. 2*F*–*I*). In control astrocytes, as expected, local application of DHPG or SDF-1α evoked an increase in the frequency and in the amplitude of sub-plasmalemmal Ca^{2+} events (Fig. 2*G*,*H*, Supplementary Fig. 3*F*,*G*). Temporal distribution of individual Ca^{2+} events gave rise to a biphasic burst comprising 2 phases: a rapid one peaking at ~200 ms and a slower one peaking at ~400 ms after stimulation (Fig. 2*I*). The overexpression of Homer1b significantly increased the frequency but not the amplitude of sub-plasmalemmal Ca^{2+} events (Fig. 2*G*,*H*) and gave rise to a biphasic burst with faster peaks (~100 ms and ~250 ms, respectively, Fig. 2*I*). Conversely, the presence of Homer1a significantly decreased the frequency and the amplitude of sub-plasmalemmal Ca^{2+} events and gave rise to a dramatic change of the temporal distribution (Fig. 2*F*,*I*); no rapid biphasic burst was observed, just a small group of localized Ca^{2+} events peaking at 500 ms. Thus Homer1a, likely by preventing ER tubules to approach the plasma membrane, caused a dramatic reduction of the sub-plasmalemmal Ca^{2+} events and, consequently, a general dysregulation of the global GPCR/ER-mediated Ca^{2+} signaling in astrocytes.

Reactive Astrocytes Upregulate Homer1a

In neurons Homer1a expression is significantly increased in several neurological disorders characterized by a strong neuroinflammatory component, such as chronic inflammatory pain or traumatic brain injury (Miyabe et al. 2006; Tappe et al. 2006; Luo et al. 2014). Beyond neurons however, it is widely accepted that inflammatory processes involve primarily astrocytes that become active (or "reactive") and undergo morphological and functional changes (Pekny and Pekna 2014). We thus investigated the expression of Homer1 proteins in astrocytes under inflammatory conditions. Cultured astrocytes, similarly to astrocytes in tissues, expressed substantial levels of Homer1b/c and almost undetectable levels of Homer1a (Supplementary Fig. 4*A*). Interestingly, when cells were long-term treated with pathological concentrations of the proinflammatory mediator tumor necrosis factor-α (TNFα, 30 ng/mL), the levels of Homer1a significantly increased (Supplementary Fig. 4*A*). Moreover, in such astrocytes the activation of mGlu1/5 elicited Ca^{2+} signals (Supplementary Fig. 4*B*,*C*) with amplitudes similar to those previously determined in cells overexpressing Homer1a. We then moved to the in vivo situation by taking advantage of the Rice–Vannucci rat HI model, a well-established paradigm of acute brain injury that recapitulates most of the inflammatory processes occurring in perinatal human cerebral HI, including the activation of astrocytes (Rice et al. 1981; Vannucci and Hagberg 2004; Gelot et al. 2009). We evaluated the expression of Homer proteins in the ipsilateral cortex of sham-operated and HI rats, 24 h and one week after HI. As assessed by immunoperoxidase labeling and western blotting analysis, the expression of the Homer1 protein variants showed opposite trends: while Homer1a reached a peak in the lesion border at 7 days, Homer1b/c significantly decreased starting from the first day after the injury (Fig. 3A; Supplementary Fig. 5*A*). GFAP, which elevated levels represent a general marker of astrocytic activation (Eng et al. 2000), recapitulated well the Homer1a expression, peaking at 7 days after the injury especially in the border of the lesion (Fig. 3*B*; Supplementary Fig. 5*A*). Confocal analysis allowed us to determine the cell types expressing Homer1a and Homer1b/c by showing a relatively low signal both in neurons and astrocytes at 1 day and an elevated signal confined in GFAP-positive astrocytes at 7 days after HI (Fig. 3*C*, Supplementary Fig. 5*B*–*E*). The astrocytes expressing Homer1a were hypertrophic reactive cells mainly located in the scarred area surrounding the lesion. Astrocytes from sham-operated animals did not express detectable amounts of Homer1a (Supplementary Fig. 6*A*,*B*). Interestingly, the upregulation of Homer1a in reactive astrocytes was not specific to a postnatal HI injury. Indeed, reactive astrocytes from ischemic tissues of adult mice subjected to intraluminal middle cerebral artery occlusion (MCAO) exhibited a similar pattern of expression (Supplementary Fig. 6*C*,*D*). Furthermore, we assessed whether these results could be translated to the human brain in normal and pathological conditions. We analyzed the GFAP/Homer1 changes in the cerebral cortex of both control and human newborns that died after birth from perinatal asphyxia. In controls, the cerebral cortex was characterized by a scarce presence of reactive astrocytes (Fig. 3*D*) whereas in hypoxia-ischemic encephalopathy (HIE) cases, the cerebral cortex displayed prominent GFAP immunoreactivity throughout cortical layers and white matter (Fig. 3*E*). Consistent with GFAP immunoreactivity, confocal analysis of the cerebral cortex of control newborns revealed an imperceptible Homer1a signal, which, instead, was readily detectable and mostly localized in reactive astrocytes of cerebral cortex from HIE human newborns.

Reactive Astrocytes Display Reduced Cytosolic Ca^{2+} Signaling and Loss of Confined Ca^{2+} Activities in Response to mGlu5 Activation

Given the selective localization of Homer1a in the reactive astrocytes at 7 days after the ischemic insult, we next investigated the

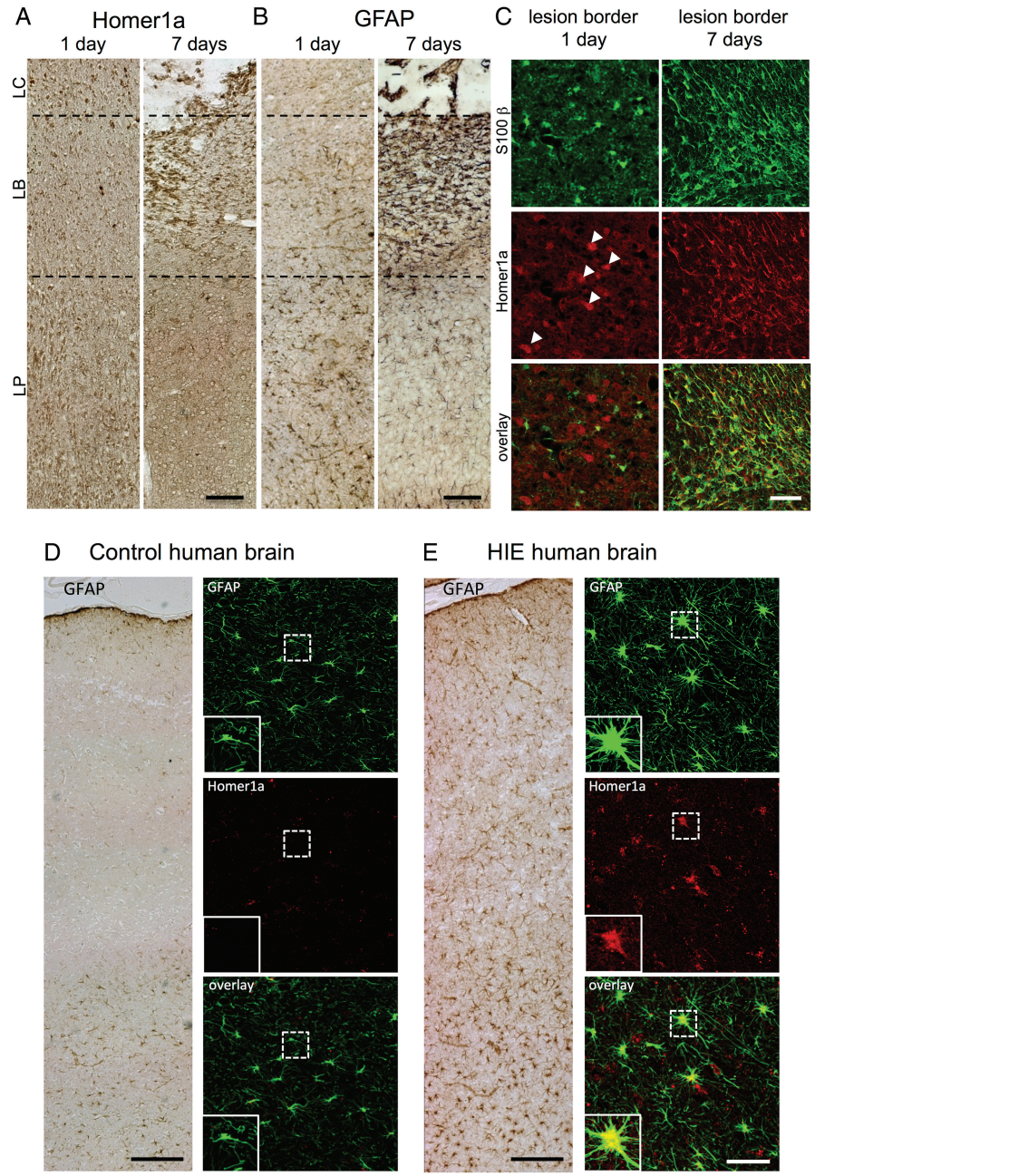

Figure 3. Reactive astrocytes upregulate Homer1a. (*A–C*) Reactive astrogliosis and Homer1a expression in a rat model of neonatal HI. (*A*) In HI animals, Homer1a immunohistochemistry staining is present in the cortical areas peripheral to the lesion (LP, lesion periphery) at 1 day after the insult. At 7 days after HI the staining is stronger in the area (LB, lesion border) adjacent to the lesion core (LC). (*B*) In ischemic animals, a mild astrocytic reaction (identified by GFAP immunohistochemistry staining) is present in the lesion periphery at 1 day after the insult. At 7 days after HI there is a gradient of reactive astrocytosis that culminates in an astrocytic scar in the lesion border. (*C*) The double immunofluorescence staining for S100β (green) and Homer1a (red) shows that at 1 day after HI, Homer1a expression is stronger in neurons (white arrowheads) than in astrocytes, whereas at 7 days postinsult Homer1a strongly overlaps with S100β-positive cells on the astrocytic scar. (*D*, *E*) Homer1a is expressed in reactive astrocytes of human HIE newborns. Left panels show representative images of GFAP immunohistochemistry staining on postmortem brain sections of human newborn controls (*D*) and HIE (*E*) cases. In the right panels, images of GFAP (green) and Homer1a (red) immunofluorescence costaining in consecutive brain sections of the same control (*D*) or HIE (*E*) case illustrate that Homer1a expression is largely increased and concurrent with reactive astrocytes in HIE newborns. Insets (bottom-left side of immunofluorescence images) show higher magnification of selected astrocytes (white boxes). Fluorescence images are z-stack maximal projections. Scale bars: (*A*, *B*) 100 μm, (*C*) 50 μm, (*D*, *E*) 200 μm (immunohistochemistry), 50 μm (immunofluorescence).

relevance of Homer1a expression for mGlu5-evoked Ca^{2+} signaling in astrocytes located in the area surrounding the lesion. We hypothesized that the expression of Homer1a in reactive astrocytes would weaken their mGlu1/5-dependent Ca^{2+} signaling, as already reported in cultured astrocytes overexpressing Homer1a (Fig. 2*C–I*). To measure mGlu1/5-dependent Ca^{2+} signaling in tissue, acute slices from the ipsilateral cortex of sham-operated and HI rats at 7 days after injury were loaded with the Ca^{2+} dye Fluo-4 acetoxymethyl ester (Fluo-4 AM) and sulforhodamine 101 (SR101), a specific marker of astrocytes (Nimmerjahn et al. 2004). After bulk loading, de-esterified Fluo-4 was incorporated almost exclusively into SR101-positive astrocytes (Hirase et al.

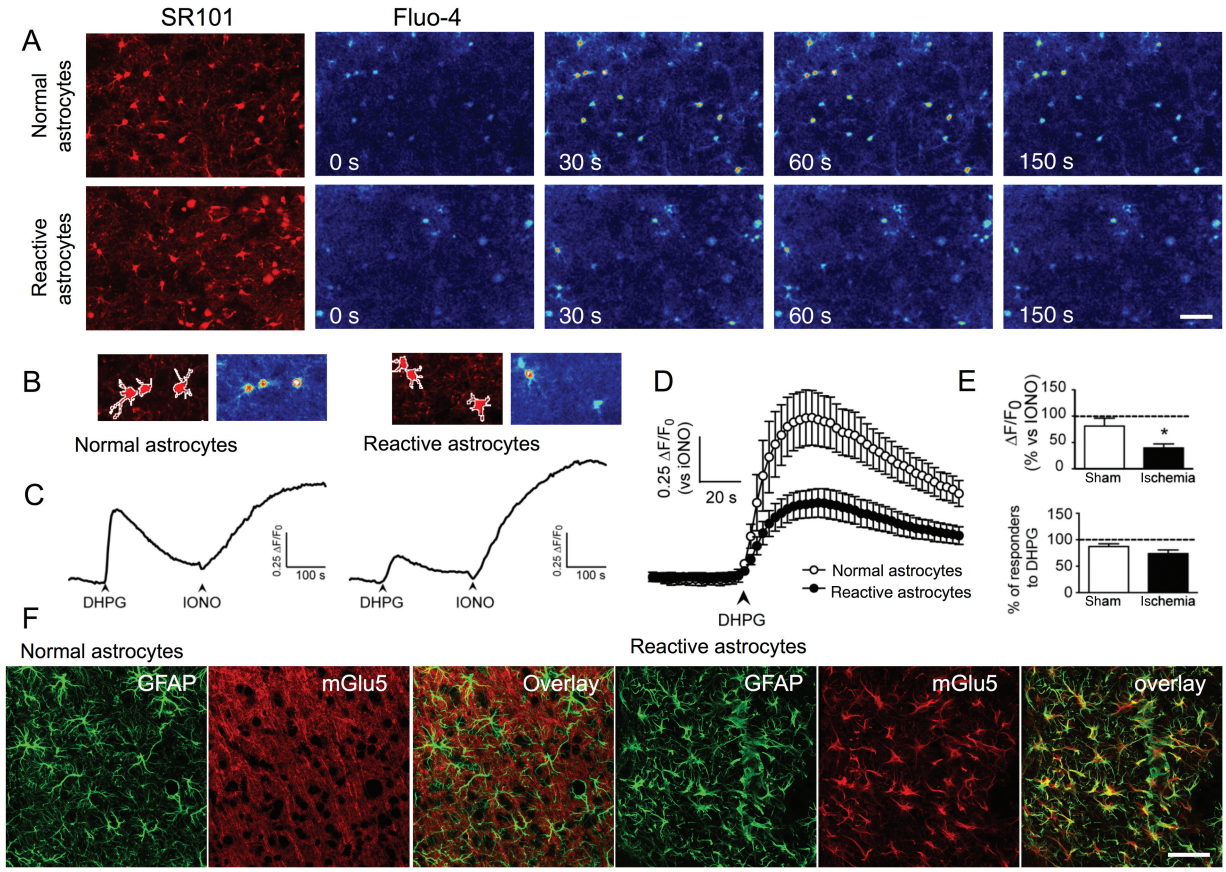

Figure 4. Global Ca^{2+} response evoked by mGlu1/5 stimulation is impaired in reactive astrocytes from ischemic tissue. (*A*) At 7 days after induction of HI, acute brain slices (250 μm, coronal) are incubated 60 min at 34°C in aCSF with the Ca^{2+} indicator Fluo-4 AM (10 μM) and the specific astrocytic marker sulforhodamine 101 (SR101, 2 μM) and subsequently washed for 20 min. The left panels show the SR101 (red) stained astrocytes. The series of sequential images in pseudo color illustrate typical examples of the evolution of Fluo-4 fluorescence intensity induced by application of the group I mGluR agonist DHPG (100 μM) on tissue from sham-operated (normal astrocytes, top) or HI (reactive astrocytes, bottom) animals. (*B*) To analyze the global Ca^{2+} response of astrocytes, ROIs outlining the cell bodies and the large processes of SR101-positive cells are defined and their Fluo-4 intensity changes are monitored and expressed as $\Delta F/F_0$. (*C*) Representative traces of the $[Ca^{2+}]_i$ increases after application of DHPG and ionomycin (IONO, 10 μM), which is used as positive control, on slices from sham-operated and HI animals (left and right, respectively) as shown in (*B*). (*D*) The time-course of the average % of $\Delta F/F_0$ normalized to the maximal ionomycin response shows a decrease in the maximal amplitude of the response to DHPG in reactive astrocytes ($n = 5$ animals, 7 slices, approximately 250 cells for sham; $n = 5$ animals, 10 slices, approximately 250 cells for HI, mean ± SEM per slice). (*E*) The amplitude of the response to DHPG in reactive astrocytes is significantly reduced ($P = 0.015$, unpaired Student's *t*-test) while no discernable change in the number of responding cells is observed ($P = 0.187$, Mann–Whitney *U*-test). (*F*) The immunostaining of GFAP (green) and mGlu5 (red) in sham animals (left panels) and in HI animals (right panels) shows the increased and extensive expression of mGlu5 at 7 days after the ischemic insult in reactive astrocytes from the area bordering the lesion (*z*-stack maximum projection). Scale bars: 50 μm. Asterisks indicate significant differences between groups (*$P < 0.05$, unpaired Student's *t*-test).

2004; Gomez-Gonzalo et al. 2010) of both sham-operated and ischemic tissues (Fig. 4A). We monitored the changes in $[Ca^{2+}]_i$ in response to DHPG application (100 μM) in populations of normal and reactive astrocytes of sham-operated or HI cortex by keeping confocal lasers at the weakest possible power levels while maintaining good signal-to-noise ratios. In all the recordings, normal and reactive astrocytes generated spontaneous Ca^{2+} activities during a stable baseline of about 50 s (about 1 oscillation/min). Global astrocytic $[Ca^{2+}]_i$ changes induced by a bath application of DHPG were analyzed by placing ROIs around the cell body and large processes of SR101-positive astrocytes (Fig. 4B). DHPG-induced significant Ca^{2+} responses in the majority of normal and reactive astrocytes (87.20 ± 5.27% of responders in sham, 73.88 ± 6.70% of responders in ischemia, Fig. 4C–E). Figure 4D shows baseline-subtracted and normalized $[Ca^{2+}]_i$ levels from normal and reactive astrocytes. The peaks of the Ca^{2+} responses were smaller in reactive astrocytes than those in normal astrocytes (−50.3%, Fig. 4E). Interestingly, immunolabeling experiments excluded that the decreased Ca^{2+} responses in astrocytes were due to a reduction in mGlu5 expression because reactive astrocytes located in the scarred area surrounding the lesion showed a strong mGlu5 expression (Fig. 4F). Further experiments revealed that in ischemic tissues from adult mice subjected to MCAO the activation of astrocytes was accompanied by a strong mGlu5 expression (Supplementary Fig. 6D), as already reported in other neuroinflammatory conditions (Drouin-Ouellet et al. 2011; Martorana et al. 2012).

Recent findings highlighted that besides the global Ca^{2+} signals, astrocytic processes exhibit localized Ca^{2+} increases, which, at least in part, are evoked by activation of GPCRs including mGlu1/5 and depend on inositol-1,4,5-trisphosphate (InsP3) Ca^{2+} release from astrocytic internal stores (Di Castro et al. 2011; Panatier et al. 2011). We, thus, explored the effects of Homer proteins on localized mGlu-mediated Ca^{2+} signaling in astrocytic processes. For analysis, we focused on single astrocytes clearly showing a cellular segment favorably lying in the focal plane and comprising parts both of the soma and a main astrocytic process (Fig. 5A,C), as already reported (Di Castro et al. 2011). Ca^{2+} signals have been evaluated by subdividing soma and process in equal-sized (~1 μm^2) ROIs (Fig. 5A,C),

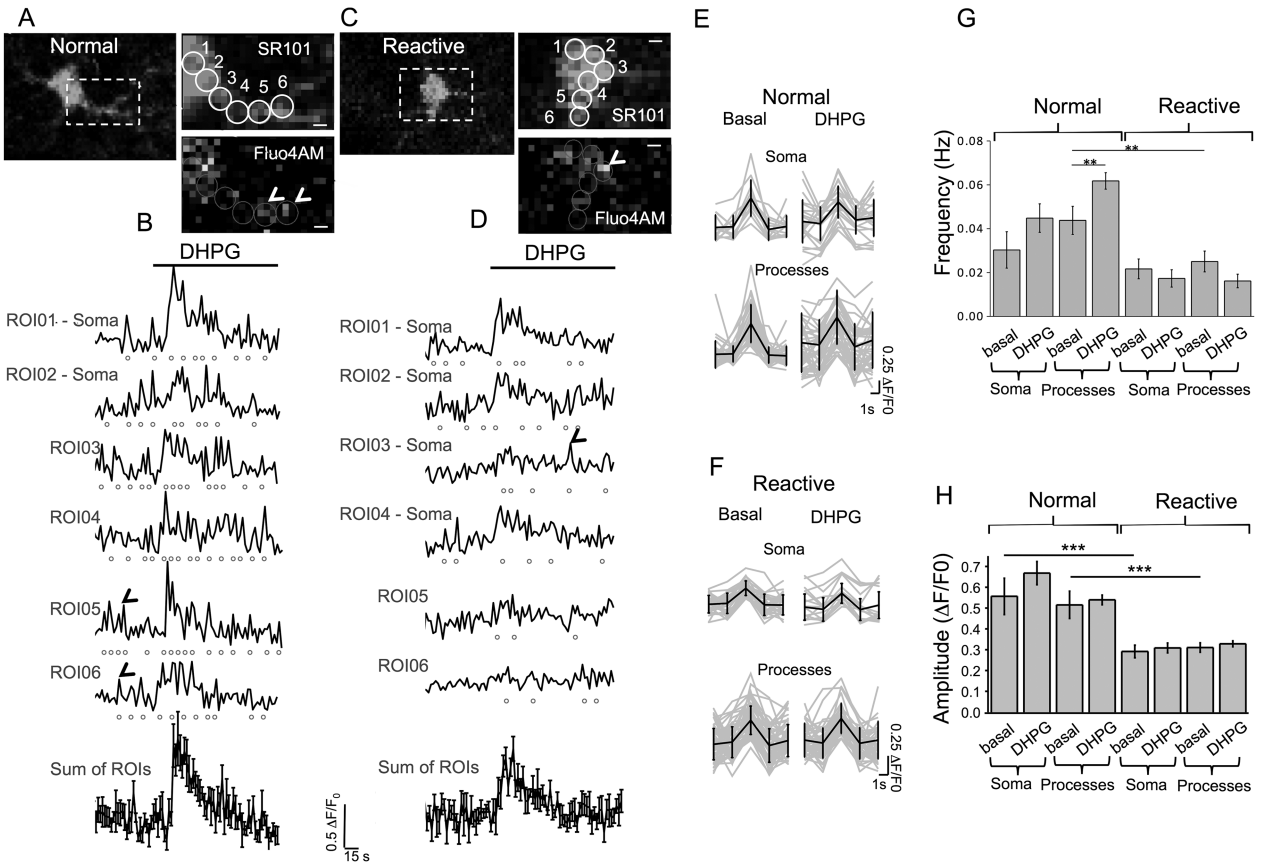

Figure 5. Local Ca^{2+} response evoked by mGlu1/5 stimulation is impaired in reactive astrocytes from ischemic tissue. (*A*) SR101-positive astrocytes responsive to DHPG are selected (left) from slices of healthy rats and ROI (1 μm^2) are placed on the cell body and along the main process (right). Dashed box (left) indicates the location of the insets (right). The ROIs are placed starting on the soma and numbered according to their distance from the initial point. Ca^{2+} signals (grayscale images) in each ROI underwent measurable rises and falls as shown in the traces in (*B*); dots underneath represent each detected Ca^{2+} spike. Two localized Ca^{2+} signals seen in (*A*) are highlighted with arrowheads in the respective ROI traces. DHPG application causes an elevation in global Ca^{2+} signal as seen in each trace as a positive deviation from the background level, and changes of some parameters of localized Ca^{2+} spikes (quantified in *G* and *F*). Scale bars: 800 nm (*C*, *D*) Analysis of reactive astrocytes is shown as in (*A*, *B*), with fewer and smaller localized Ca^{2+} responses (*D*) compared with their healthy counterparts. Mean traces with standard errors (*B*, *D* bottom) represent the sum of ROIs and show a pattern of global $[Ca^{2+}]_i$ change (see Fig. 4*D* for comparison). Localized Ca^{2+} events of normal (*E*) and reactive (*F*) astrocytes are pooled together and are shown grouped based on their location (soma/process) and stimulation (basal/DHPG). Black bold traces in each of the aggregates represent the mean localized events ± SD. Frequency (*G*) and amplitude (*H*) of identified localized events are measured under basal conditions and after DHPG challenge, and are split into events occurring in the somata and processes of normal and reactive astrocytes. Asterisks indicate significant differences between groups [$^*P < 0.05$, $^{**}P < 0.01$, $^{***}P < 0.001$, unpaired Student *t*-test (normal vs. reactive) or one-way ANOVA with Bonferroni post-test (within normal or reactive)].

which correspond approximately to the surface of a cluster formed by mGluR5 and Homer1b/c, as seen in Figure 1*E–F* and Supplementary Figure 2. The Ca^{2+} traces obtained from each ROI were expressed as $\Delta F/F_0$, where F_0 is the mean of at least 6 s of the basal level (Fig. 5*B*,*D*). At first, we defined the temporal characteristics of the localized Ca^{2+} signals. Although our sampling rate was slow when analyzing the Ca^{2+} traces, we could identify many "spike-like" events clearly distinguishable from the background (Fig. 5*B*,*D*). The spike-like events were spatially confined in a surface of about 1.2 µm and occurred both in the soma and in the processes with similar amplitudes and kinetics (last ~4 s and peak at ~2 s, Fig. 5*E*,*F*). We determined that the spatially confined Ca^{2+} events occurred more often in the processes with respect to the soma (Fig. 5*G*), as already reported (Haustein et al. 2014). Application of DHPG (40 µM) transiently increased the global Ca^{2+} levels as expected (Fig. 5*B*), without preventing the identification of confined Ca^{2+} signals in the individual ROIs. DHPG did not alter the amplitude and kinetics of the confined events (Fig. 5*E–H*), but significantly increased their frequency by about 40% (1 event/20s/ROI vs 1.4 events/20s/ROI) (Fig. 5*G*). In reactive astrocytes, the situation was dramatically different. The cells showed hypertrophy and a relative shortening of their processes (Fig. 5*C*). Confined Ca^{2+} signals both from soma and processes showed a dramatic decrease in their amplitudes and frequencies with respect to normal astrocytes (–44% of amplitude, –37% of frequency, Fig. 5*G*,*H*). In reactive astrocytes, the application of DHPG caused a small increase of global Ca^{2+} (Fig. 5*D*) but did not elicit any change in amplitudes and frequencies of confined Ca^{2+} signals (Fig. 5*F–H*). Overall, the analyses of Ca^{2+} dynamics in vitro and in situ strongly suggest that Homer1 proteins play a crucial role in modulating mGlu1/5 Ca^{2+} signaling.

Homer1a Exerts a Strong Control on Glutamate Release From Astrocytes

Glutamatergic gliotransmission, defined as the Ca^{2+}-dependent and regulated release of glutamate by astrocytes upon activation of Gq GPCRs, including mGlu1/5 (Bezzi and Volterra 2001; Araque et al. 2014; Petrelli and Bezzi 2016), is implicated in rapid synaptic communication in the brain (Haydon 2001; Volterra and

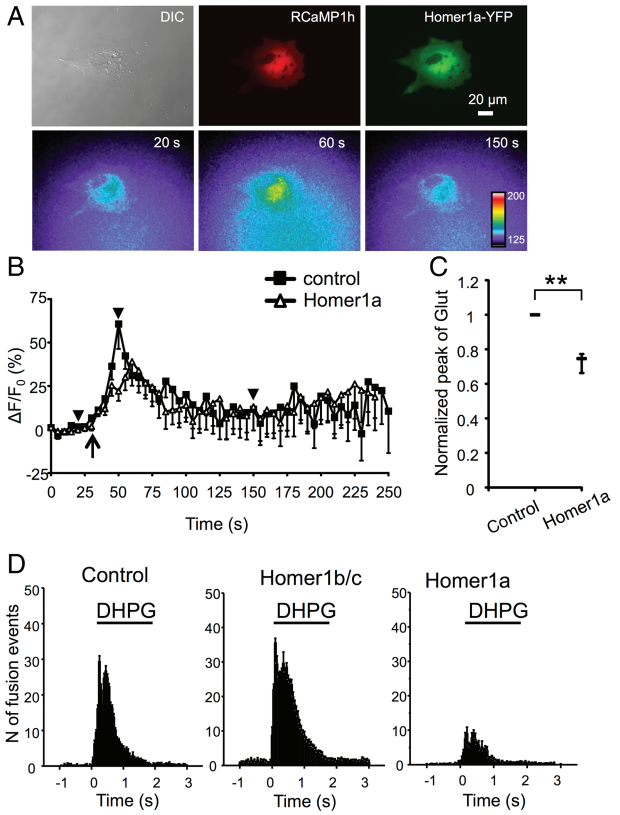

Figure 6. Homer1a reduces exocytotic glutamate release from astrocytes. (*A*) Differential interference contrast (DIC) image (top left) of a solitary astrocyte coexpressing RCaMP1h (top center, red) and Homer1a-YFP (top right, green). The lower panels show NADH fluorescence images, reporting on extracellular glutamate surrounding somata of solitary astrocytes, taken at different time points (black arrowheads in *B*) before and after mechanical stimulation (indicated by an arrow in *B*). The pseudo color scale is a linear representation of the fluorescence intensity ranging from 125 to 200 intensity units. (*B*) Average kinetics of extracellular NADH fluorescence (means ± SEM) in solitary astrocytes expressing either RCaMP1h alone (control, black squares, $n = 15$ cells) or along with Homer1a-YFP (open triangles, $n = 15$ cells) in response to mechanical stimulation (arrow). Changes in NADH fluorescence are shown as % $\Delta F/F_0$ after background subtraction and correction for bleaching. SEMs are shown in single direction for clarity. (*C*) Normalized peak of glutamate (Glut) release; dashes represent medians with interquartile range and asterisks indicate significant changes (**$P < 0.01$, Mann–Whitney *U*-test). Scale bar: 20 µm. (*D*) Temporal distribution of fusion events of VGLUT1-pHluorin expressing vesicles evoked by DHPG application (2 s, 100 µM) in control cells and in cells overexpressing Homer1a-CFP. Each individual histogram represents the number (mean ± SEM) of fusion evens detected in a 50-ms-long frame ($n = 8$ cells). (*E*) Frequency histograms of VGLUT1-pHluorin events in control cells and in cells transfected with Homer1a-CFP. Note that overexpression of Homer1a significantly decreases the frequency of fusion events. (**$P < 0.01$, one-way ANOVA).

Meldolesi 2005; Perea et al. 2009; Santello and Volterra 2009). Therefore, we next asked whether abnormal Ca^{2+} signaling in reactive astrocytes might have a consequence on the glutamate gliosecretory process. We turned to studies in cell cultures, where mGlu1/5 activation was established to trigger glutamate release via Ca^{2+}-dependent vesicular exocytosis (Bezzi et al. 2001; Cali et al. 2014) and where cellular and molecular mechanisms can be readily studied (Montana et al. 2004; Marchaland et al. 2008; Shigetomi and Khakh 2009; Bergersen et al. 2012). Our first question was whether the presence of Homer1a could disrupt Ca^{2+}-dependent release of glutamate from astrocytes. To this purpose, we optically monitored glutamate release into the medium surrounding cultured astrocytes transfected with Homer1a-YFP and/or RCaMP1h constructs by taking advantage of the glutamate dehydrogenase (GDH) linked assay (Hua et al. 2004). This fluorescent assay for glutamate released by cultured cells is based on the accumulation of the fluorescent product NADH in the extracellular space surrounding astrocytes (Montana et al. 2004). To evoke Ca^{2+}-dependent glutamate release from astrocytes, we used mechanical stimulation, known to cause an increase in astrocytic intracellular Ca^{2+} levels leading to glutamate release (Parpura et al. 1994; Araque et al. 1998; Montana et al. 2004) (Supplementary Fig. 3A–C). To apply a gentle mechanical stimulation, we established a contact between the transfected astrocytes and the patch pipette under the control of a patch-clamp amplifier (Montana et al. 2004). The mechanical stimulation caused glutamate release from astrocytes with or without exogenous Homer1a-YFP expression (Fig. 6A–B). Consistent with a smaller amplitude of $[Ca^{2+}]_i$ peak (−29%; $P < 0.01$, Mann–Whitney *U*-test; Supplementary Fig. 3A–C) imaging data, the glutamate released from astrocytes overexpressing Homer1a was significantly reduced with respect to control cells (−25%; $P < 0.01$, Mann–Whitney *U*-test) (Fig. 6C). We then went to investigate whether Homer1a influenced the signaling process leading to glutamate exocytosis from astrocytes. To this end, we used a specific marker of glutamatergic vesicle exocytosis, VGLUT1-pHluorin, the chimerical fluorescent protein formed by vesicular glutamate transporter-1 (VGLUT1) coupled to a modified version of GFP sensitive to the change in proton concentration (pHluorin) (Voglmaier et al. 2006; Balaji and Ryan 2007; Marchaland et al. 2008). We evoked exocytosis in cells with or without overexpression of Homer1a by stimulating mGlu1/5 with DHPG (100 µM, 2 s), as already reported (Marchaland et al. 2008). As expected, in control cells DHPG evoked a biphasic burst of exocytotic events (348 ± 13.16 events; $n = 7$) occurring in strict temporal correlation with sub-plasmalemmal Ca^{2+} events with 2 peaks of exocytosis, each one slightly following the corresponding peak of Ca^{2+} (first peak at ~250 ms from the start of the stimulus and the second peak at ~450 ms, Fig. 6D). In astrocytes overexpressing Homer1a, the effect of DHPG on exocytosis of VGLUT1-positive vesicles was dramatically different. Consistent with an impairment of the sub-plasmalemmal Ca^{2+} signaling, we found a significant decrease in the number of exocytotic events (121 ± 8.6 events; $n = 8$;—65%, Fig. 6D) and a dramatic slow-down of the release process. Thus, in the presence of Homer1a, glutamate exocytosis was dramatically impaired, further confirming that Homer1 proteins act on the mGluR5 Ca^{2+} signaling to modify the gliosecretory properties of astrocytes.

SiRNA Knockdown of Homer1a in Reactive Astrocytes Exacerbates Both Ca^{2+} Signals and Glutamate Release and Sensitizes Astrocytes to Apoptosis

To further investigate the role of Homer1a expression in reactive astrocytes, we knocked down Homer1a mRNA using short interfering RNA (siRNA)-mediated depletion (Supplementary Fig. 7A; Moutin et al. 2012; Serchov et al. 2015). The in vitro evaluation of the siRNAs efficacy in cultured primary astrocytes revealed about 40% downregulation of TNFα-induced Homer1a mRNA levels by siRNA2 at 48 h after delivery (Supplementary Fig. 7B). The siRNA2 was further selected for in vivo intracerebroventricular microinjections, since it also decreased TNFα-induced Homer1a protein levels in vitro at 72 h after its delivery (Supplementary Fig. 7C). The siRNA2 was also powerful in inhibiting the effects of Homer1a upregulation on DHPG-induced Ca^{2+} signals and glutamate exocytosis (Supplementary Fig. 7D–E) in cultured astrocytes treated with a pathological concentration of TNFα. To

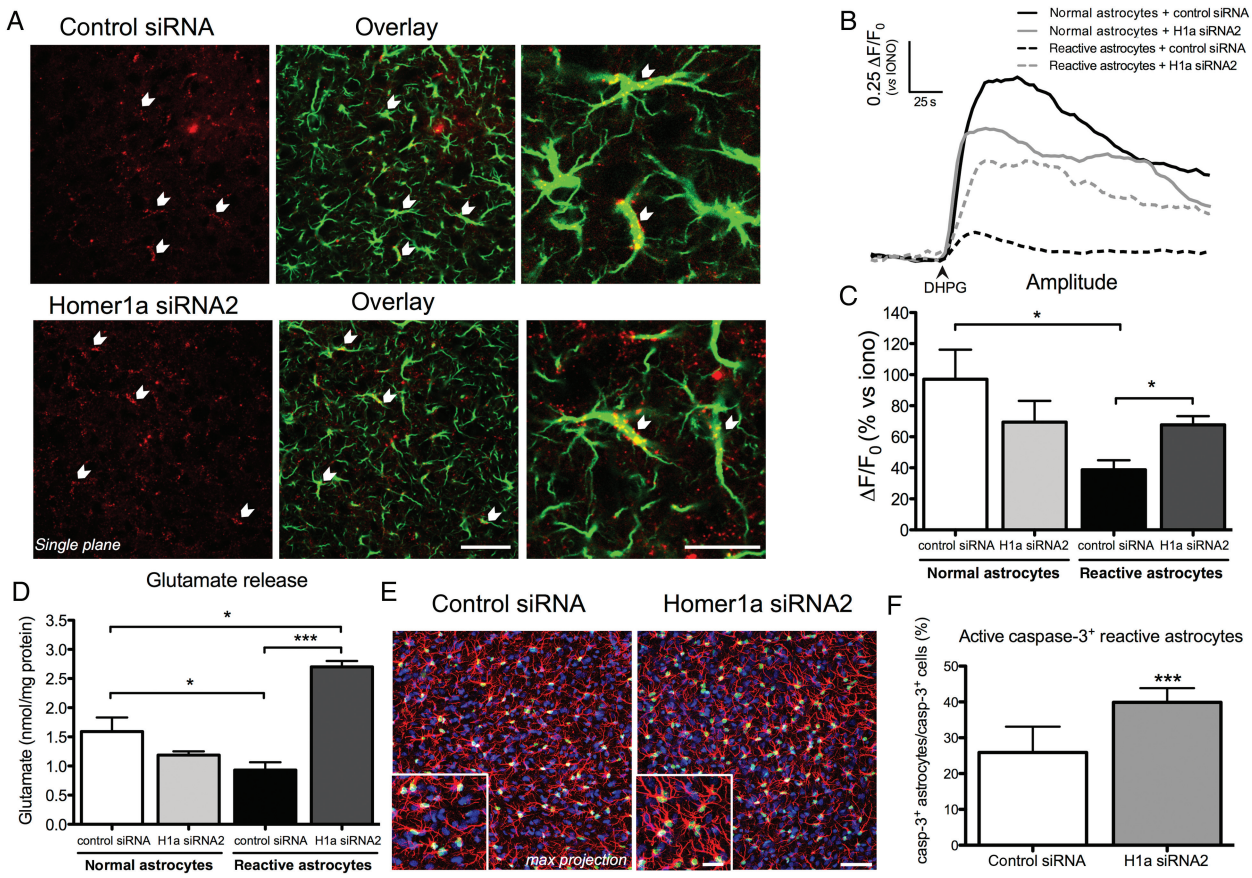

Figure 7. Effects of Homer1a knockdown on reactive astrocytes. (*A*) Intracerebroventricularly delivered nontargeting control siRNA and anti-Homer1a siRNA2 (red) are present in GFAP-positive reactive astrocytes (green) 2 days after the injection, as seen in single plane confocal images (high magnification shown in right panels) (*B*) Representative $\Delta F/F_0$, normalized to the maximal ionomycin response, time-course traces of DHPG-stimulated normal and reactive astrocytes in acute slices from animals injected with nontargeting control siRNA or anti-Homer1a siRNA2. (*C*) The amplitude of DHPG-evoked intracellular Ca^{2+} transients is significantly smaller in control siRNA-treated reactive astrocytes than in control siRNA-treated normal astrocytes and is restored by the knockdown of Homer1a with siRNA2 (mean ± SEM, $n = 3$ animals, 3 slices per condition). (*D*) Acute slices from siRNA-injected sham- or HI-operated rats are incubated with bafilomycin A1 and stimulated with DHPG to induce the release of extracellular glutamate from astrocytes. In slices from ischemic animals injected with control siRNA ($n = 6$) the release of extracellular glutamate is significantly smaller than in slices from sham animals ($n = 5$). The knockdown of Homer1a with siRNA2 on slices from ischemic animals ($n = 3$) significantly amplified the extracellular glutamate release from astrocytes (mean ± SEM). (*E*) Immunofluorescence analysis of tissue from HI animals injected with control siRNA or anti-Homer1a siRNA2 reveals the presence of GFAP-positive (red) reactive astrocytes that immunopositive for the active form of caspase-3 (green). (*F*) Quantification of active caspase-3 positive reactive astrocytes shows that the knockdown of Homer1a with siRNA2 increases the number of active caspase-3 positive reactive astrocytes (mean ± SD, $n = 3$ animals). (*$P < 0.05$, ***$P < 0.001$, unpaired Student's *t*-test and one-way ANOVA with Bonferroni's post-test). Scale bars: 50 μm (low magnification) and 20 μm (higher magnification).

test the effects of Homer1a in reactive astrocytes in vivo, we injected siRNA2 in the ipsilateral ventricle of sham-operated and HI rats 5 days after the surgery (Fig. 7*A*), a period characterized by a significant increase of mGlu5 and of Homer1a in reactive astrocytes (Fig. 3*A*,*B*, Fig. 4*F*). The mGlu1/5 Ca^{2+}-signaling was then checked in control siRNA- or siRNA2-containing reactive astrocytes 2 days after the injection (one week after HI) by confocal Ca^{2+} imaging in acute slices challenged with DHPG. Consistent with previous data (Fig. 4*D*,*E*), reactive astrocytes expressing control siRNA showed a substantial decrease in the amplitude of cytoplasmic Ca^{2+} signals with respect to normal astrocytes of sham-operated rats injected with control siRNA (–60% of sham injected with control siRNA, Fig. 7*B*,*C*). Homer1a knockdown restored in reactive astrocytes the amplitude of DHPG-evoked Ca^{2+} transients (–34% of sham injected with control siRNA, Fig. 7*B*, *C*). siRNA2 also directly affected glutamate release by astrocytes in situ (Fig 7*D*). Acute slices from sham-operated and HI rats incubated with bafilomycin A1 (BafA1), a blocker of vesicular/exocytotic release of glutamate from neuronal terminals (Zhou et al. 2000), were stimulated with DHPG (100 μM) to induce glutamate release from astrocytes. BafA1 (2 μM) abolished glutamate release by synaptic terminals induced by high K^+ (KCl, 20 mM) (–96%, $n = 3$) within 2 h, a time frame in which the drug does not affect astrocyte transmitter release in hippocampal slices (Domercq et al. 2006; Di Castro et al. 2011). Consistent with previous reports (Bezzi et al. 2001; Domercq et al. 2006), application of DHPG in acute slices from sham-operated rats injected with control siRNA induced the release of extracellular glutamate, even in the absence of glutamate exocytosis from synaptic terminals (Fig. 7*D*). The release of extracellular glutamate was, however, significantly smaller from slices taken form ischemic animals with respect to sham (–39% of sham injected with control siRNA, Fig. 7*D*), thus confirming the effect of Homer1a on glutamate exocytosis in vitro (Fig. 6). Knockdown of Homer1a with siRNA2 amplified glutamate release from slices taken from ischemic animals (+80% of sham injected with control siRNA, Fig. 7*D*), with minimal effects on sham slices (Fig. 7*D*) and confirmed once more the effect in vitro (Fig. 6). Finally, because a role for mGlu5-mediated

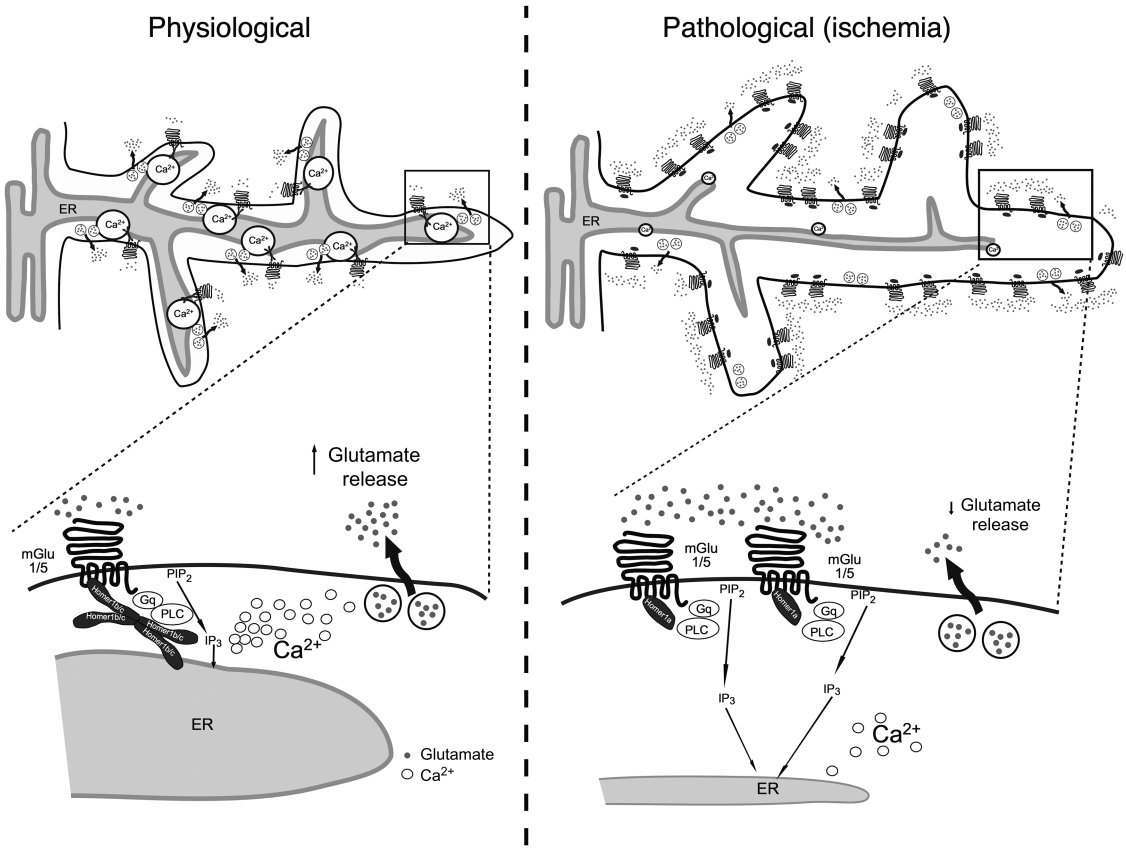

Figure 8. Working model. Under physiological conditions (left), astrocytes transduce an extracellular signal (glutamate, blue dots) through the membrane-bound mGlu1/5 receptor into the cell. In the cytoplasm, the mGlu1/5 receptor is physically linked to Homer1b/c oligomers and, through them, to the ER. This tether enhances the vicinity of the Ca^{2+}-containing ER and together with the Ca^{2+}-sensitive exocytotic machinery forms a functionally relevant structural microdomain. Under pathological conditions (right) Homer1b/c is replaced by its nonoligomerizing splice variant Homer1a, which lacks the coiled-coil domain and thus prevents the formation of mGlu1/5-Homer1-ER clusters. As a consequence of this and together with the fact that astrocytes under ischemic condition undergo hypertrophy, the transduction is impaired and very little Ca^{2+} is immediately available in these functional domains on both local and global levels to fuel processes such as gliotransmission.

Ca^{2+} signaling was identified in the gliodegenerative processes of reactive astrocytes (Rossi et al. 2008; Martorana et al. 2012), we investigated the effect of Homer1a knockdown on the morphological and structural changes of reactive astrocytes. While we could not find any difference in terms of gross anatomical abnormalities such as amount of cells expressing GFAP (17.2 ± 2.2% in HI siRNA2 vs 17.3 ± 4.5% in HI control siRNA) or morphology of GFAP-positive cells (Fig. 7*E*), immunofluorescence analysis revealed an increased number of reactive astrocytes immunopositive for the active form of caspase-3, cleaved caspase-3 (39.9 ± 4.0% in HI siRNA2 vs 25.9 ± 7.2% in HI control siRNA, Fig. 7*E*,*F*), a widely used marker of apoptosis and cell death (Nicholson et al. 1995). Taken together, these data suggest that astroglial Homer1a increased expression could be crucial for limiting Ca^{2+}-mediated cell death in reactive astrocytes.

Discussion

Here, we show that Homer1b/c is constitutively expressed in astrocytes, where it clusters with mGlu5 and ER tubules to form sub-plasmalemmal microdomains. The presence of Homer1b/c in astrocytic processes facilitates global and highly localized GPCR-mediated Ca^{2+} signaling, the main intracellular pathway regulating the release of gliotransmitters. In reactive astrocytes, Homer1b/c is replaced by Homer1a, hindering the physical link between mGlu5 and the ER and limiting the efficacy of mGlu5 Ca^{2+} signaling and thus limiting the extent of gliodegeneration (Fig. 8).

The long coiled-coil encoding forms of the scaffolding protein Homer1 are constitutively expressed in many brain regions including cerebral cortex and are enriched in dendritic spines at the postsynaptic density, where they contribute to maintaining the architecture of signaling complexes (Tu et al. 1999; Xiao et al. 2000; Hayashi et al. 2009). In dendritic spines, they function as a physical link between plasmalemma-bound group I mGlus and ER-located IP_3Rs (Tu et al. 1998) and, consequently, they ensure the spatial proximity of the signal transduction machinery to the Ca^{2+} stores (Sala et al. 2005). Here, we show evidence that Homer1b/c is constitutively expressed in developing astrocytes of murine cortical tissues. Our results are in consonance with the RNA-sequencing transcriptome database, where cortical astrocytes were found positive for Homer1 (Zhang et al. 2014). Homer1b/c immunoreactivity was visible in the soma and main processes as well as in the perivascular end feet of astrocytes, emphasizing the widespread distribution of this scaffold protein across cellular compartments. At the subcellular level, both Homer 1b/c and mGlu5 presented a punctate distribution that was reminiscent of that of the mGlu5 immunostaining pattern along astrocytic processes recently shown in adult astrocytes (Panatier et al. 2011). Further analysis performed in cultured cells as well as in astrocytic processes in situ revealed that Homer1b/c recruited mGlu5 at the plasma membrane and

partially colocalized with the receptor by forming clusters of about 1 μm in diameter. By analogy with dendritic spines, Homer1b/c-mGlu5 clusters would then define the sites of structural microdomains housing the membrane receptors and the downstream Ca^{2+} machinery in astrocytes. Consistently, cultured astrocytes (over)expressing Homer1b/c had a significant amount of ER tubules lying in the sub-plasmalemmal area.

What could be the functional meaning of such clusters in astrocytes? In neurons, Homer1 proteins can modulate Ca^{2+} signaling by determining the physical proximity of the plasmalemmal mGlu5 to IP_3 receptors on the ER tubules (Xiao et al. 1998). The present study addresses for the first time the role of Homer1 proteins in the mGlu5-mediated Ca^{2+} responses in astrocytes. By employing single-cell imaging techniques in cultured and in situ astrocytes we found that Homer1 proteins governed the spatiotemporal characteristics of Ca^{2+} events in astrocytes. In cultured astrocytes the overexpression of the long and short forms of Homer1 proteins had opposite results. Homer1b/c facilitated the occurrence of highly localized sub-plasmalemmal Ca^{2+} events and optimized their temporal distribution in response to the activation of the receptor, an effect consistent with the formation of clusters with plasmalemma-bound mGlu1/5 and ER tubules. Homer1a, instead, dramatically reduced the frequency and the magnitude of sub-plasmalemmal Ca^{2+} events and disrupted the efficacy of mGlu1/5 signaling in causing a synchronized burst of events. In normal astrocytic processes in situ, those expressing Homer1b/c in basal conditions, we found spatially confined Ca^{2+} events. Such events occurred mainly in the processes with respect to the soma, as already reported (Haustein et al. 2014), and showed an average surface (about $1\mu m^2$) compatible with that of mGlu5-Homer1b/c clusters. Their amplitude and kinetics were not only blocked by depleting intracellular Ca^{2+} stores (data not shown), thus reminding the pharmacology of the elementary Ca^{2+} "puffs" produced by the opening of clusters of IP_3Rs in neurons (Koizumi et al. 1999; Delmas and Brown 2002), but were also increased by the agonist DHPG, thus pointing out their mGlu1/5-dependency. From the subcellular point of view, the presence of localized Ca^{2+} events implies the presence of localized Ca^{2+} stores and thus of subcellular specializations within individual astrocytic compartments (for review, (Rusakov et al. 2014)). Electron microscopy studies have indeed indicated that astrocyte architecture is characterized by the prevalence of processes containing ER tubules (Bezzi et al. 2004; Pivneva et al. 2008; Bergersen et al. 2012). This architecture could favor the organization of subcellular structural domains (Blaustein and Golovina 2001; Rusakov et al. 2014) similar to those already described in dendritic spines (Yuste et al. 2000) and support the generation of highly localized Ca^{2+} signals (Llinas et al. 1995; Berridge 2006; Rizzuto and Pozzan 2006). In reactive Homer1a-expressing astrocytic processes, we found a dramatic reduction in the basal frequency of spatially confined events and almost no response to the mGlu1/5 agonist. The absence of localized Ca^{2+} events was consistent with TIRF data showing the absence of ER tubules at the submembrane domains in cells overexpressing Homer1a. Interestingly, by analyzing the effects of Homer1 proteins at the global cellular level we noticed that Ca^{2+} responses in the cytosol (both amplitude and temporal kinetics) were directly correlated with the number of localized Ca^{2+} events. For instance, in the case of Homer1a overexpression, the drop in localized events corresponded with a strong reduction of cytosolic Ca^{2+} signaling. Thus, one can speculate that localized Ca^{2+} events, probably originating from the putative structural microdomains, might act as "pacemakers" for Ca^{2+}-induced Ca^{2+} release (CICR; Koizumi et al. 1999) and consequently drive global Ca^{2+} responses. In this scenario, the localized Ca^{2+} events would be at the origin of global Ca^{2+} transients, but what would then be the source of such localized events in the first place? The existence of global spontaneous astrocytic Ca^{2+} oscillations independent of neuronal activity in the early postnatal period was already reported (Parri et al. 2001). These spontaneous oscillations were dependent on intracellular Ca^{2+} stores (Parri et al. 2001) and more precisely, on IP_3R-induced Ca^{2+} release from ER stores (Wang, Zhou; et al. 2006). However, other sources of Ca^{2+} could also be at the origin of the local spontaneous events. In fact, it has been recently observed that highly localized spontaneous Ca^{2+} elevations under the astrocytic membrane were partly dependent on transmembrane Ca^{2+} fluxes (Srinivasan et al. 2015) and mediated by transient receptor potential ankyrin 1 (TRPA1) channels (Shigetomi et al. 2012). The localized Ca^{2+} elevations in astrocytes in basal conditions may also arise therefore from an influx of extracellular Ca^{2+} across the plasma membrane through the opening of TRPA1 channels. Moreover, TRPA1 can be gated by robust activation of the PLC pathway (Bandell et al. 2004), which happens after stimulation of Gq-GPCRs, therefore contributing to the increase in amplitude and frequency of the local Ca^{2+} events in response to DHPG, a response facilitated by the enhanced proximity of the ER Ca^{2+} store mediated by Homer1b/c. We could also consider TRPA1 channel opening as a source of Ca^{2+} that could account for the sparse local Ca^{2+} events occurring in the presence of Homer1a. Interestingly, activation of group I mGluR using DHPG also recruits store-operated calcium entry via TRP canonical 1 (TRPC1)-containing plasmalemmal channels in astrocytes (Malarkey et al. 2008). This raises an issue of possible multiple plasmalemmal entities that could be involved in the proposed signaling scheme.

Our study suggests that the functional roles of Homer1b/c-mGlu1/5 clusters go beyond a simply permissive effect on the detection of neuronal activity. Indeed, the organization of such structurally defined subcellular microdomains could effectively transduce specific, localized signals to tailored outputs, such as the release of gliotransmitters from astrocytes. We found that Homer1 proteins, while exerting a tight control on Ca^{2+} signaling, influence astrocytic glutamate release. We have previously shown that the exocytotic burst of glutamatergic vesicles correlates in time with sub-membrane Ca^{2+} events evoked by activation of mGlu1/5 (Marchaland et al. 2008; Cali et al. 2014). Here we show that, compared with control cells, in cultured astrocytes overexpressing Homer1a as well as in Homer1a-positive reactive astrocytes in situ the evoked vesicle fusions or glutamate release, respectively, were significantly decreased and slowed down. Analysis of the temporal distribution of fusion events in cultured astrocytes showed, in particular, a complete disappearance of the rapid phase of the exocytotic burst (0–400 ms). As this rapid phase is sustained almost exclusively by resident vesicles, that is, vesicles lying close to the plasma membrane before the stimulus (Marchaland et al. 2008), it is tempting to speculate that the structural microdomains in astrocytes comprise not only mGlu1/5-Homer1–ER but also glutamatergic vesicles. Indeed, it has been reported that the long forms of Homer1 interact via their C-terminal domains with syntaxin 12 (Minakami et al. 2000). This member of a family of proteins largely involved in docking and fusion events of vesicles has been localized, like Homer1 proteins, in small puncta in somatodendritic processes (Prekeris et al. 1999).

The existence of an mGlu1/5- and Ca^{2+}-dependent glutamate secretion process in the developing cortex confirms the competence of astrocytes to interact with synaptic activity during the assembly of synaptic circuits, as already reported (Porter and Mccarthy 1996; Pasti et al. 1997; Perea and Araque 2005; Panatier et al. 2011). It is interesting to note that in murine astrocytes

Homer1b/c is expressed as early as P5, but it does not reach the punctate pattern of expression seen in adult tissue until the age of P10, suggesting a maturation process of the structural microdomains. In fact, the period over which the modulation of Ca^{2+} signaling and the underlying glutamate release by Homer1 proteins has been observed is an important time in cortical development. It is therefore possible that glutamatergic gliotransmission plays an important role in the strengthening of synaptic connections and the establishment of neuronal pathways. There is also a possibility that the dramatic reduction of mGlu5 expression in astrocytes after this "critical period" (Sun et al. 2013) could be related to the establishment and maturation of local Ca^{2+} microdomains in astrocytes, which could be at its turn related to the establishment of preferred neuronal pathways. Indeed, some studies performed with animals past this critical period have shown that there is a response to basal synaptic activity with rapid increases in Ca^{2+} concentration in astrocytic microdomains (Panatier et al. 2011). Once these pathways are established, in the more mature brain, the decrease in the expression of mGlu5 and the local restriction of its related signaling could be an important way to strengthen the specificity of the received/processed information and also to modulate astrocyte-neuron glutamatergic signaling in order to prevent a potentially deleterious overstimulation due to a widespread gliotransmitter release. In this context, Homer1 proteins, by regulating the assembly of these structural and functional astrocytic microdomains, would play an important role. It is interesting to note that in many inflammatory brain pathologies, even in the adult brain, there is an extensive upregulation of astrocytic mGlu5. This situation, leading to the loss of the local restriction of the mGlu5- and Ca^{2+}-dependent glutamate secretion processes, reminiscent of the maturing brain scenario, could initially contribute to wreaking havoc, but properly regulated could possibly participate in the mechanisms of tissue repair.

An intriguing observation in our study is that astrocytic Homer1 proteins are modulated by pathological concentrations of proinflammatory mediators. We found that Homer1b/c was downregulated immediately after an ischemic insult whereas Homer1a was upregulated, similarly to tissues from pathologies characterized by a strong neuroinflammatory component (Tappe et al. 2006; Luo et al. 2014). Indeed, in response to TNFα astrocytic Homer1a is upregulated, which in turn limits astrocytic Ca^{2+} signaling and glutamate release. The latter appears to be in discordance with our previous observation of enhanced astrocytic glutamate release upon exposure to TNFα (Bezzi et al. 2001; Santello et al. 2011). However, this paradox can be resolved if we consider the different time scales involved; while acute TNFα exposure led to fast glutamate release (Bezzi et al. 2001; Santello et al. 2011) longer exposure to the cytokine was associated with a slower glutamate release (Figs 6 and 7). We hypothesize that an increased expression of Homer1a could be an integral part of an adaptive/regulatory mechanism to avoid the potential deleterious effects of an excessive extracellular glutamate concentration due to a sustained TNFα activation.

In keeping with Homer1a being protective, others have shown that TNFα/cycloheximide induced a Homer1a increase that protected from apoptosis (Luo et al. 2012). Many studies have shown that the Ca^{2+}-dependent intracellular signaling activated by mGlu1/5 was implicated in different brain disorders (Merlin 2002; Stoop et al. 2003; Giuffrida et al. 2005; Ronesi et al. 2012) including those associated with the presence of reactive astrocytes (Tappe et al. 2006; Rossi et al. 2008; Martorana et al. 2012). In many of such disorders, the role of Homer1a was mainly neuroprotective through a negative regulation of mGlu1/5 signaling (Tappe et al. 2006; Ronesi et al. 2012; Luo et al. 2014). A recent study also described the role of mGlu5-signaling and Homer1 proteins in the protection of astrocytes from apoptosis (Paquet et al. 2013). Our discovery that Homer1a was responsible for much of the downregulation of mGlu1/5 Ca^{2+} signaling and glutamate release in reactive astrocytes is in line with such recent results and strongly suggests that the Homer1a upregulation in hypertrophic reactive astrocytes may represent a protective mechanism to limit the intensity and the duration of the mGlu1/5 activation. Indeed, such reactive astrocytes were located around the focal ischemic region constituting a border between the lesion and the surrounding brain tissues where reactive astrogliosis is severe and leads to glial scar formation (Sofroniew and Vinters 2010; Sofroniew 2015). Taking into consideration that reactive astrogliosis might have unique cellular and molecular characteristics in different neuropathologies (Pekny and Pekna 2014), the astrocytic scars might have evolved to demarcate the lesion and temporarily or permanently separate it from the surrounding inflammatory cells and infectious agents (Sofroniew and Vinters 2010). It is noteworthy that the glial scar formation is associated with substantive tissue reorganization that is long lasting and persists long after the insult. The fact that downregulation of Homer1a sensitizes to apoptosis a subset of reactive astrocytes mainly confined to the glial scar border, suggests that these particular reactive cells should have a particular function and impact on neonatal HI. As the changes undergone during reactive astrogliosis have the potential to alter astrocyte activities both through gain and loss of functions that can impact both beneficially and detrimentally on surrounding neural and non-neural cells, taken together, our data point toward a crucial importance of the scaffold protein Homer1a to favor the survival of surrounding cells.

Our study describes that Homer1a by limiting the spreading of toxic glutamatergic gliotransmission may be one of the cellular mechanisms developed by reactive astrocytes to protect neighboring cells (both astrocytes and neurons) in pathological conditions characterized by high levels of TNFα. In view of these considerations, therapeutic agents targeting the astrocytic mGlu5-mediated signaling, as recently done for amyotrophic lateral sclerosis (Martorana et al. 2012), could be tested against neurodegeneration and cognitive disturbances in such clinical conditions.

Supplementary Material

Supplementary Material can be found at http://www.cercor.oxfordjournals.org/ online.

Funding

This work was supported by Swiss National Foundation, National Centres of Competence in Research (NCCR) "Synapsy" and "TransCure" to P.B., by Swiss National Science Foundation (310030-135617/1) to L.H. and P.B., by Swiss National Science Foundation (310030-130769 and 310030-163064) to J.P. and A.-T., by National Institutes of Health (The Eunice Kennedy Shriver National Institute of Child Health and Human Development award HD078678) to V.P., Comitato Telethon Fondazione Onlus, grant GGP11095 and Ministry for Education, University and Research, Project of National Interest (PRIN) 2010-2011 to C.S. *Conflict of Interest*: None declared.

Notes

We thank R.H. Edwards (UCSF) for providing the VGLUT1-pHluorin; H. Kettenmann (Max Delbrück Center) for providing

GFAP-EGFP mice; Jean Daraspe of the Electron Microscopy Facility (University of Lausanne) and the Cellular Imaging Facility (University of Lausanne) for technical and experimental support.

References

Agulhon C, Fiacco TA, McCarthy KD. 2010. Hippocampal short- and long-term plasticity are not modulated by astrocyte Ca2 + signaling. Science. 327:1250–1254.

Akerboom J, Carreras Calderon N, Tian L, Wabnig S, Prigge M, Tolo J, Gordus A, Orger MB, Severi KE, Macklin JJ, et al. 2013. Genetically encoded calcium indicators for multi-color neural activity imaging and combination with optogenetics. Front Mol Neurosci. 6:2.

Ango F, Pin JP, Tu JC, Xiao B, Worley PF, Bockaert J, Fagni L. 2000. Dendritic and axonal targeting of type 5 metabotropic glutamate receptor is regulated by homer1 proteins and neuronal excitation. J Neurosci. 20:8710–8716.

Ango F, Prezeau L, Muller T, Tu JC, Xiao B, Worley PF, Pin JP, Bockaert J, Fagni L. 2001. Agonist-independent activation of metabotropic glutamate receptors by the intracellular protein Homer. Nature. 411:962–965.

Araque A, Carmignoto G, Haydon PG, Oliet SH, Robitaille R, Volterra A. 2014. Gliotransmitters travel in time and space. Neuron. 81:728–739.

Araque A, Parpura V, Sanzgiri RP, Haydon PG. 1998. Glutamate-dependent astrocyte modulation of synaptic transmission between cultured hippocampal neurons. Eur J Neurosci. 10:2129–2142.

Attwell D, Buchan AM, Charpak S, Lauritzen M, Macvicar BA, Newman EA. 2010. Glial and neuronal control of brain blood flow. Nature. 468:232–243.

Balaji J, Ryan TA. 2007. Single-vesicle imaging reveals that synaptic vesicle exocytosis and endocytosis are coupled by a single stochastic mode. Proc Natl Acad Sci U S A. 104:20576–20581.

Bandell M, Story GM, Hwang SW, Viswanath V, Eid SR, Petrus MJ, Earley TJ, Patapoutian A. 2004. Noxious cold ion channel TRPA1 is activated by pungent compounds and bradykinin. Neuron. 41:849–857.

Bergersen LH, Morland C, Ormel L, Rinholm JE, Larsson M, Wold JF, Roe AT, Stranna A, Santello M, Bouvier D, et al. 2012. Immunogold detection of L-glutamate and D-serine in small synaptic-like microvesicles in adult hippocampal astrocytes. Cereb Cortex. 22:1690–1697.

Berridge MJ. 2006. Calcium microdomains: organization and function. Cell Calcium. 40:405–412.

Bezzi P, Carmignoto G, Pasti L, Vesce S, Rossi D, Rizzini BL, Pozzan T, Volterra A. 1998. Prostaglandins stimulate calcium-dependent glutamate release in astrocytes. Nature. 391:281–285.

Bezzi P, Domercq M, Brambilla L, Galli R, Schols D, De Clercq E, Vescovi A, Bagetta G, Kollias G, Meldolesi J, et al. 2001. CXCR4-activated astrocyte glutamate release via TNFalpha: amplification by microglia triggers neurotoxicity. Nat Neurosci. 4:702–710.

Bezzi P, Gundersen V, Galbete JL, Seifert G, Steinhauser C, Pilati E, Volterra A. 2004. Astrocytes contain a vesicular compartment that is competent for regulated exocytosis of glutamate. Nat Neurosci. 7:613–620.

Bezzi P, Volterra A. 2001. A neuron-glia signalling network in the active brain. Curr Opin Neurobiol. 11:387–394.

Blaustein MP, Golovina VA. 2001. Structural complexity and functional diversity of endoplasmic reticulum Ca(2+) stores. Trends Neurosci. 24:602–608.

Brakeman PR, Lanahan AA, O'Brien R, Roche K, Barnes CA, Huganir RL, Worley PF. 1997. Homer: a protein that selectively binds metabotropic glutamate receptors. Nature. 386: 284–288.

Cali C, Lopatar J, Petrelli F, Pucci L, Bezzi P. 2014. G-protein coupled receptor-evoked glutamate exocytosis from astrocytes: role of prostaglandins. Neural Plast. 2014:254574.

Clarke LE, Barres BA. 2013. Emerging roles of astrocytes in neural circuit development. Nat Rev Neurosci. 14:311–321.

Coutinho V, Kavanagh I, Sugiyama H, Tones MA, Henley JM. 2001. Characterization of a metabotropic glutamate receptor type 5-green fluorescent protein chimera (mGluR5-GFP): pharmacology, surface expression, and differential effects of Homer-1a and Homer-1c. Mol Cell Neurosci. 18:296–306.

Delmas P, Brown DA. 2002. Junctional signaling microdomains: bridging the gap between the neuronal cell surface and Ca2+ stores. Neuron. 36:787–790.

Demaurex N, Frieden M. 2003. Measurements of the free luminal ER Ca(2+) concentration with targeted "cameleon" fluorescent proteins. Cell Calcium. 34:109–119.

Di Castro MA, Chuquet J, Liaudet N, Bhaukaurally K, Santello M, Bouvier D, Tiret P, Volterra A. 2011. Local Ca2+ detection and modulation of synaptic release by astrocytes. Nat Neurosci. 14:1276–1284.

Domercq M, Brambilla L, Pilati E, Marchaland J, Volterra A, Bezzi P. 2006. P2Y1 receptor-evoked glutamate exocytosis from astrocytes: control by tumor necrosis factor-alpha and prostaglandins. J Biol Chem. 281:30684–30696.

Drouin-Ouellet J, Brownell AL, Saint-Pierre M, Fasano C, Emond V, Trudeau LE, Levesque D, Cicchetti F. 2011. Neuroinflammation is associated with changes in glial mGluR5 expression and the development of neonatal excitotoxic lesions. Glia. 59:188–199.

Eng LF, Ghirnikar RS, Lee YL. 2000. Glial fibrillary acidic protein: GFAP-thirty-one years (1969–2000). Neurochem Res. 25:1439–1451.

Eroglu C, Barres BA. 2010. Regulation of synaptic connectivity by glia. Nature. 468:223–231.

Fagni L, Chavis P, Ango F, Bockaert J. 2000. Complex interactions between mGluRs, intracellular Ca2+ stores and ion channels in neurons. Trends Neurosci. 23:80–88.

Fellin T, Pascual O, Gobbo S, Pozzan T, Haydon PG, Carmignoto G. 2004. Neuronal synchrony mediated by astrocytic glutamate through activation of extrasynaptic NMDA receptors. Neuron. 43:729–743.

Fiacco TA, Agulhon C, Taves SR, Petravicz J, Casper KB, Dong X, Chen J, McCarthy KD. 2007. Selective stimulation of astrocyte calcium in situ does not affect neuronal excitatory synaptic activity. Neuron. 54:611–626.

Gelot A, Villapol S, Billette de Villemeur T, Renolleau S, Charriaut-Marlangue C. 2009. Astrocytic demise in the developing rat and human brain after hypoxic-ischemic damage. Dev Neurosci. 31:459–470.

Giaume C, Koulakoff A, Roux L, Holcman D, Rouach N. 2010. Astroglial networks: a step further in neuroglial and gliovascular interactions. Nat Rev Neurosci. 11:87–99.

Ginet V, Pittet MP, Rummel C, Osterheld MC, Meuli R, Clarke PG, Puyal J, Truttmann AC. 2014. Dying neurons in thalamus of asphyxiated term newborns and rats are autophagic. Ann Neurol. 76:695–711.

Ginet V, Puyal J, Clarke PG, Truttmann AC. 2009. Enhancement of autophagic flux after neonatal cerebral hypoxia-ischemia and its region-specific relationship to apoptotic mechanisms. Am J Pathol. 175:1962–1974.

Girouard H, Bonev AD, Hannah RM, Meredith A, Aldrich RW, Nelson MT. 2010. Astrocytic endfoot Ca2+ and BK channels

determine both arteriolar dilation and constriction. Proc Natl Acad Sci U S A. 107:3811–3816.

Giuffrida R, Musumeci S, D'Antoni S, Bonaccorso CM, Giuffrida-Stella AM, Oostra BA, Catania MV. 2005. A reduced number of metabotropic glutamate subtype 5 receptors are associated with constitutive homer proteins in a mouse model of fragile X syndrome. J Neurosci. 25:8908–8916.

Gomez-Gonzalo M, Losi G, Chiavegato A, Zonta M, Cammarota M, Brondi M, Vetri F, Uva L, Pozzan T, de Curtis M, et al. 2010. An excitatory loop with astrocytes contributes to drive neurons to seizure threshold. PLoS Biol. 8:e1000352.

Gordon GR, Choi HB, Rungta RL, Ellis-Davies GC, MacVicar BA. 2008. Brain metabolism dictates the polarity of astrocyte control over arterioles. Nature. 456:745–749.

Halassa MM, Fellin T, Takano H, Dong JH, Haydon PG. 2007. Synaptic islands defined by the territory of a single astrocyte. J Neurosci. 27:6473–6477.

Halassa MM, Haydon PG. 2010. Integrated brain circuits: astrocytic networks modulate neuronal activity and behavior. Annu Rev Physiol. 72:335–355.

Haustein MD, Kracun S, Lu XH, Shih T, Jackson-Weaver O, Tong X, Xu J, Yang XW, O'Dell TJ, Marvin JS, et al. 2014. Conditions and constraints for astrocyte calcium signaling in the hippocampal mossy fiber pathway. Neuron. 82:413–429.

Hayashi MK, Tang C, Verpelli C, Narayanan R, Stearns MH, Xu RM, Li H, Sala C, Hayashi Y. 2009. The postsynaptic density proteins Homer and Shank form a polymeric network structure. Cell. 137:159–171.

Haydon PG. 2001. GLIA: listening and talking to the synapse. Nat Rev Neurosci. 2:185–193.

Henneberger C, Papouin T, Oliet SH, Rusakov DA. 2010. Long-term potentiation depends on release of D-serine from astrocytes. Nature. 463:232–236.

Hirase H, Qian L, Bartho P, Buzsaki G. 2004. Calcium dynamics of cortical astrocytic networks in vivo. PLoS Biol. 2:E96.

Honsek SD, Walz C, Kafitz KW, Rose CR. 2012. Astrocyte calcium signals at Schaffer collateral to CA1 pyramidal cell synapses correlate with the number of activated synapses but not with synaptic strength. Hippocampus. 22:29–42.

Hua X, Malarkey EB, Sunjara V, Rosenwald SE, Li WH, Parpura V. 2004. C(a2+)-dependent glutamate release involves two classes of endoplasmic reticulum Ca(2+) stores in astrocytes. J Neurosci Res. 76:86–97.

Iadecola C, Nedergaard M. 2007. Glial regulation of the cerebral microvasculature. Nat Neurosci. 10:1369–1376.

Inoue Y, Honkura N, Kato A, Ogawa S, Udo H, Inokuchi K, Sugiyama H. 2004. Activity-inducible protein Homer1a/Vesl-1S promotes redistribution of postsynaptic protein Homer1c/Vesl-1L in cultured rat hippocampal neurons. Neurosci Lett. 354:143–147.

Jaiswal JK, Simon SM. 2007. Imaging single events at the cell membrane. Nat Chem Biol. 3:92–98.

Kammermeier PJ. 2006. Surface clustering of metabotropic glutamate receptor 1 induced by long Homer proteins. BMC Neurosci. 7:1.

Koizumi S, Bootman MD, Bobanovic LK, Schell MJ, Berridge MJ, Lipp P. 1999. Characterization of elementary Ca2+ release signals in NGF-differentiated PC12 cells and hippocampal neurons. Neuron. 22:125–137.

Lavialle M, Aumann G, Anlauf E, Prols F, Arpin M, Derouiche A. 2011. Structural plasticity of perisynaptic astrocyte processes involves ezrin and metabotropic glutamate receptors. Proc Natl Acad Sci U S A. 108:12915–12919.

Lee CJ, Mannaioni G, Yuan H, Woo DH, Gingrich MB, Traynelis SF. 2007. Astrocytic control of synaptic NMDA receptors. J Physiol. 581:1057–1081.

Lee W, Malarkey EB, Reyes RC, Parpura V. 2008. Micropit: a New cell culturing approach for characterization of solitary astrocytes and small networks of these glial cells. Front Neuroeng. 1:2.

Levine S. 1960. Anoxic-ischemic encephalopathy in rats. Am J Pathol. 36:1–17.

Llinas R, Sugimori M, Silver RB. 1995. The concept of calcium concentration microdomains in synaptic transmission. Neuropharmacology. 34:1443–1451.

Luo P, Chen T, Zhao Y, Zhang L, Yang Y, Liu W, Li S, Rao W, Dai S, Yang J, et al. 2014. Postsynaptic scaffold protein Homer 1a protects against traumatic brain injury via regulating group I metabotropic glutamate receptors. Cell Death Dis. 5:e1174.

Luo P, Zhao Y, Li D, Chen T, Li S, Chao X, Liu W, Zhang L, Qu Y, Jiang X, et al. 2012. Protective effect of Homer 1a on tumor necrosis factor-alpha with cycloheximide-induced apoptosis is mediated by mitogen-activated protein kinase pathways. Apoptosis. 17:975–988.

Malarkey EB, Ni Y, Parpura V. 2008. Ca2+ entry through TRPC1 channels contributes to intracellular Ca2+ dynamics and consequent glutamate release from rat astrocytes. Glia. 56:821–835.

Marchaland J, Cali C, Voglmaier SM, Li H, Regazzi R, Edwards RH, Bezzi P. 2008. Fast subplasma membrane Ca2+ transients control exo-endocytosis of synaptic-like microvesicles in astrocytes. J Neurosci. 28:9122–9132.

Martorana F, Brambilla L, Valori CF, Bergamaschi C, Roncoroni C, Aronica E, Volterra A, Bezzi P, Rossi D. 2012. The BH4 domain of Bcl-X(L) rescues astrocyte degeneration in amyotrophic lateral sclerosis by modulating intracellular calcium signals. Hum Mol Genet. 21:826–840.

Menard C, Quirion R. 2012. Successful cognitive aging in rats: a role for mGluR5 glutamate receptors, homer 1 proteins and downstream signaling pathways. PLoS One. 7:e28666.

Merlin LR. 2002. Differential roles for mGluR1 and mGluR5 in the persistent prolongation of epileptiform bursts. J Neurophysiol. 87:621–625.

Min R, Nevian T. 2012. Astrocyte signaling controls spike timing-dependent depression at neocortical synapses. Nat Neurosci. 15:746–753.

Minakami R, Kato A, Sugiyama H. 2000. Interaction of Vesl-1L/Homer 1c with Syntaxin 13. Biochem Biophys Res Commun. 272:466–471.

Miyabe T, Miletic G, Miletic V. 2006. Loose ligation of the sciatic nerve in rats elicits transient up-regulation of Homer1a gene expression in the spinal dorsal horn. Neurosci Lett. 398:296–299.

Montana V, Ni Y, Sunjara V, Hua X, Parpura V. 2004. Vesicular glutamate transporter-dependent glutamate release from astrocytes. J Neurosci. 24:2633–2642.

Moutin E, Raynaud F, Roger J, Pellegrino E, Homburger V, Bertaso F, Ollendorff V, Bockaert J, Fagni L, Perroy J. 2012. Dynamic remodeling of scaffold interactions in dendritic spines controls synaptic excitability. J Cell Biol. 198:251–263.

Navarrete M, Perea G, Fernandez de Sevilla D, Gomez-Gonzalo M, Nunez A, Martin ED, Araque A. 2012. Astrocytes mediate in vivo cholinergic-induced synaptic plasticity. PLoS Biol. 10: e1001259.

Nicholson DW, Ali A, Thornberry NA, Vaillancourt JP, Ding CK, Gallant M, Gareau Y, Griffin PR, Labelle M, Lazebnik YA, et al. 1995. Identification and inhibition of the ICE/CED-3 protease necessary for mammalian apoptosis. Nature. 376:37–43.

Nimmerjahn A, Kirchhoff F, Kerr JN, Helmchen F. 2004. Sulforhodamine 101 as a specific marker of astroglia in the neocortex in vivo. Nat Methods. 1:31–37.

Nolte C, Matyash M, Pivneva T, Schipke CG, Ohlemeyer C, Hanisch UK, Kirchhoff F, Kettenmann H. 2001. GFAP promoter-controlled EGFP-expressing transgenic mice: a tool to visualize astrocytes and astrogliosis in living brain tissue. Glia. 33:72–86.

Panatier A, Vallee J, Haber M, Murai KK, Lacaille JC, Robitaille R. 2011. Astrocytes are endogenous regulators of basal transmission at central synapses. Cell. 146:785–798.

Paquet M, Ribeiro FM, Guadagno J, Esseltine JL, Ferguson SS, Cregan SP. 2013. Role of metabotropic glutamate receptor 5 signaling and homer in oxygen glucose deprivation-mediated astrocyte apoptosis. Mol Brain. 6:9.

Parpura V, Basarsky TA, Liu F, Jeftinija K, Jeftinija S, Haydon PG. 1994. Glutamate-mediated astrocyte-neuron signalling. Nature. 369:744–747.

Parri HR, Gould TM, Crunelli V. 2001. Spontaneous astrocytic Ca2+ oscillations in situ drive NMDAR-mediated neuronal excitation. Nat Neurosci. 4:803–812.

Pasti L, Volterra A, Pozzan T, Carmignoto G. 1997. Intracellular calcium oscillations in astrocytes: a highly plastic, bidirectional form of communication between neurons and astrocytes in situ. J Neurosci. 17:7817–7830.

Paukert M, Agarwal A, Cha J, Doze VA, Kang JU, Bergles DE. 2014. Norepinephrine controls astroglial responsiveness to local circuit activity. Neuron. 82:1263–1270.

Pekny M, Pekna M. 2014. Astrocyte reactivity and reactive astrogliosis: costs and benefits. Physiol Rev. 94:1077–1098.

Perea G, Araque A. 2007. Astrocytes potentiate transmitter release at single hippocampal synapses. Science. 317:1083–1086.

Perea G, Araque A. 2005. Properties of synaptically evoked astrocyte calcium signal reveal synaptic information processing by astrocytes. J Neurosci. 25:2192–2203.

Perea G, Navarrete M, Araque A. 2009. Tripartite synapses: astrocytes process and control synaptic information. Trends Neurosci. 32:421–431.

Petravicz J, Fiacco TA, McCarthy KD. 2008. Loss of IP3 receptor-dependent Ca2+ increases in hippocampal astrocytes does not affect baseline CA1 pyramidal neuron synaptic activity. J Neurosci. 28:4967–4973.

Petrelli F, Bezzi P. 2016. Novel insights into gliotransmitters. Curr Opin Pharmacol. 26:138–145.

Pivneva T, Haas B, Reyes-Haro D, Laube G, Veh RW, Nolte C, Skibo G, Kettenmann H. 2008. Store-operated Ca2+ entry in astrocytes: different spatial arrangement of endoplasmic reticulum explains functional diversity in vitro and in situ. Cell Calcium. 43:591–601.

Porter JT, McCarthy KD. 1996. Hippocampal astrocytes in situ respond to glutamate released from synaptic terminals. J Neurosci. 16:5073–5081.

Prekeris R, Foletti DL, Scheller RH. 1999. Dynamics of tubulovesicular recycling endosomes in hippocampal neurons. J Neurosci. 19:10324–10337.

Reyes RC, Verkhratsky A, Parpura V. 2013. TRPC1-mediated Ca2+ and Na+ signalling in astroglia: differential filtering of extracellular cations. Cell Calcium. 54:120–125.

Rice JE 3rd, Vannucci RC, Brierley JB. 1981. The influence of immaturity on hypoxic-ischemic brain damage in the rat. Ann Neurol. 9:131–141.

Rizzuto R, Pozzan T. 2006. Microdomains of intracellular Ca2+: molecular determinants and functional consequences. Physiol Rev. 86:369–408.

Ronesi JA, Collins KA, Hays SA, Tsai NP, Guo W, Birnbaum SG, Hu JH, Worley PF, Gibson JR, Huber KM. 2012. Disrupted Homer scaffolds mediate abnormal mGluR5 function in a mouse model of fragile X syndrome. Nat Neurosci. 15:431–440, S431.

Rossi D, Brambilla L, Valori CF, Roncoroni C, Crugnola A, Yokota T, Bredesen DE, Volterra A. 2008. Focal degeneration of astrocytes in amyotrophic lateral sclerosis. Cell Death Differ. 15:1691–1700.

Rusakov DA, Bard L, Stewart MG, Henneberger C. 2014. Diversity of astroglial functions alludes to subcellular specialisation. Trends Neurosci. 37:228–242.

Sala C, Futai K, Yamamoto K, Worley PF, Hayashi Y, Sheng M. 2003. Inhibition of dendritic spine morphogenesis and synaptic transmission by activity-inducible protein Homer1a. J Neurosci. 23:6327–6337.

Sala C, Piech V, Wilson NR, Passafaro M, Liu G, Sheng M. 2001. Regulation of dendritic spine morphology and synaptic function by Shank and Homer. Neuron. 31:115–130.

Sala C, Roussignol G, Meldolesi J, Fagni L. 2005. Key role of the postsynaptic density scaffold proteins Shank and Homer in the functional architecture of Ca2+ homeostasis at dendritic spines in hippocampal neurons. J Neurosci. 25:4587–4592.

Santello M, Bezzi P, Volterra A. 2011. TNFalpha controls glutamatergic gliotransmission in the hippocampal dentate gyrus. Neuron. 69:988–1001.

Santello M, Volterra A. 2009. Synaptic modulation by astrocytes via Ca2+-dependent glutamate release. Neuroscience. 158:253–259.

Sarnat HB, Sarnat MS. 1976. Neonatal encephalopathy following fetal distress. A clinical and electroencephalographic study. Arch Neurol. 33:696–705.

Schubert V, Bouvier D, Volterra A. 2011. SNARE protein expression in synaptic terminals and astrocytes in the adult hippocampus: a comparative analysis. Glia. 59:1472–1488.

Serchov T, Clement HW, Schwarz MK, Iasevoli F, Tosh DK, Idzko M, Jacobson KA, de Bartolomeis A, Normann C, Biber K, et al. 2015. Increased signaling via adenosine A1 receptors, sleep deprivation, imipramine, and ketamine inhibit depressive-like behavior via induction of homer1a. Neuron. 87:549–562.

Shigetomi E, Bushong EA, Haustein MD, Tong X, Jackson-Weaver O, Kracun S, Xu J, Sofroniew MV, Ellisman MH, Khakh BS. 2013. Imaging calcium microdomains within entire astrocyte territories and endfeet with GCaMPs expressed using adeno-associated viruses. J Gen Physiol. 141:633–647.

Shigetomi E, Khakh BS. 2009. Measuring near plasma membrane and global intracellular calcium dynamics in astrocytes. J Vis Exp.

Shigetomi E, Kracun S, Sofroniew MV, Khakh BS. 2010. A genetically targeted optical sensor to monitor calcium signals in astrocyte processes. Nat Neurosci. 13:759–766.

Shigetomi E, Tong X, Kwan KY, Corey DP, Khakh BS. 2012. TRPA1 channels regulate astrocyte resting calcium and inhibitory synapse efficacy through GAT-3. Nat Neurosci. 15:70–80.

Sofroniew MV. 2015. Astrocyte barriers to neurotoxic inflammation. Nat Rev Neurosci. 16:249–263.

Sofroniew MV, Vinters HV. 2010. Astrocytes: biology and pathology. Acta Neuropathol. 119:7–35.

Srinivasan R, Huang BS, Venugopal S, Johnston AD, Chai H, Zeng H, Golshani P, Khakh BS. 2015. Ca(2+) signaling in astrocytes from Ip3r2(−/−) mice in brain slices and during startle responses in vivo. Nat Neurosci. 18:708–717.

Stoop R, Conquet F, Pralong E. 2003. Determination of group I metabotropic glutamate receptor subtypes involved in the frequency of epileptiform activity in vitro using mGluR1 and mGluR5 mutant mice. Neuropharmacology. 44:157–162.

Sun W, McConnell E, Pare JF, Xu Q, Chen M, Peng W, Lovatt D, Han X, Smith Y, Nedergaard M. 2013. Glutamate-dependent neuroglial calcium signaling differs between young and adult brain. Science. 339:197–200.

Takata N, Mishima T, Hisatsune C, Nagai T, Ebisui E, Mikoshiba K, Hirase H. 2011. Astrocyte calcium signaling transforms cholinergic modulation to cortical plasticity in vivo. J Neurosci. 31:18155–18165.

Tappe A, Klugmann M, Luo C, Hirlinger D, Agarwal N, Benrath J, Ehrengruber MU, During MJ, Kuner R. 2006. Synaptic scaffolding protein Homer1a protects against chronic inflammatory pain. Nat Med. 12:677–681.

Tu JC, Xiao B, Naisbitt S, Yuan JP, Petralia RS, Brakeman P, Doan A, Aakalu VK, Lanahan AA, Sheng M, et al. 1999. Coupling of mGluR/Homer and PSD-95 complexes by the Shank family of postsynaptic density proteins. Neuron. 23:583–592.

Tu JC, Xiao B, Yuan JP, Lanahan AA, Leoffert K, Li M, Linden DJ, Worley PF. 1998. Homer binds a novel proline-rich motif and links group 1 metabotropic glutamate receptors with IP3 receptors. Neuron. 21:717–726.

Vannucci SJ, Hagberg H. 2004. Hypoxia-ischemia in the immature brain. J Exp Biol. 207:3149–3154.

Voglmaier SM, Kam K, Yang H, Fortin DL, Hua Z, Nicoll RA, Edwards RH. 2006. Distinct endocytic pathways control the rate and extent of synaptic vesicle protein recycling. Neuron. 51:71–84.

Volterra A, Liaudet N, Savtchouk I. 2014. Astrocyte Ca(2)(+) signalling: an unexpected complexity. Nat Rev Neurosci. 15:327–335.

Volterra A, Meldolesi J. 2005. Astrocytes, from brain glue to communication elements: the revolution continues. Nat Rev Neurosci. 6:626–640.

Wang TF, Zhou C, Tang AH, Wang SQ, Chai Z. 2006. Cellular mechanism for spontaneous calcium oscillations in astrocytes. Acta Pharmacol Sin. 27:861–868.

Wang X, Lou N, Xu Q, Tian GF, Peng WG, Han X, Kang J, Takano T, Nedergaard M. 2006. Astrocytic Ca2+ signaling evoked by sensory stimulation in vivo. Nat Neurosci. 9:816–823.

Xiao B, Tu JC, Petralia RS, Yuan JP, Doan A, Breder CD, Ruggiero A, Lanahan AA, Wenthold RJ, Worley PF. 1998. Homer regulates the association of group 1 metabotropic glutamate receptors with multivalent complexes of homer-related, synaptic proteins. Neuron. 21:707–716.

Xiao B, Tu JC, Worley PF. 2000. Homer: a link between neural activity and glutamate receptor function. Curr Opin Neurobiol. 10:370–374.

Yuste R, Majewska A, Holthoff K. 2000. From form to function: calcium compartmentalization in dendritic spines. Nat Neurosci. 3:653–659.

Zhang Y, Chen K, Sloan SA, Bennett ML, Scholze AR, O'Keeffe S, Phatnani HP, Guarnieri P, Caneda C, Ruderisch N, et al. 2014. An RNA-sequencing transcriptome and splicing database of glia, neurons, and vascular cells of the cerebral cortex. J Neurosci. 34:11929–11947.

Zhou Q, Petersen CC, Nicoll RA. 2000. Effects of reduced vesicular filling on synaptic transmission in rat hippocampal neurones. J Physiol. 525(Pt 1):195–206.